Title

Neural EGFL like 1 as a potential pro-chondrogenic, anti-inflammatory dual-functional disease-modifying osteoarthritis drug

Permalink

https://escholarship.org/uc/item/1bs3j04m

Authors

Li, Chenshuang
Zheng, Zhong
Ha, Pin
et al.

Publication Date

2020

DOI

10.1016/j.biomaterials.2019.119541

Peer reviewed

Neural EGFL like 1 as a potential pro-chondrogenic, anti-inflammatory dual-functional disease-modifying osteoarthritis drug

Chenshuang Li[1,&], **Zhong Zheng**[1,&,*], **Pin Ha**[1], **Wenlu Jiang**[1], **Emily A. Berthiaume**[2], **Seungjun Lee**[3], **Zane Mills**[4], **Hsinchuan Pan**[1], **Eric C Chen**[1], **Jie Jiang**[5], **Cymbeline T Culiat**[6], **Xinli Zhang**[1,*], **Kang Ting**[1,*], **Chia Soo**[5,*]

[1]Division of Growth and Development, Section of Orthodontics, School of Dentistry, University of California, Los Angeles, Los Angeles, CA 90095, USA

[2]David Geffen School of Medicine, University of California, Los Angeles, Los Angeles, CA 90095, USA

[3]Department of Chemistry and Biochemistry, School of Letters and Science, University of California, Los Angeles, Los Angeles, CA 90095, USA

[4]Department of Ecology and Evolutionary Biology, University of California, Los Angeles, Los Angeles, CA 90095, USA

[5]Division of Plastic and Reconstructive Surgery and Department of Orthopaedic Surgery and the Orthopaedic Hospital Research Center, University of California, Los Angeles, Los Angeles, CA 90095, USA

[6]NellOne Therapeutics, Inc., Oak Ridge, TN 37830, USA

[*]To whom correspondence and material requests should be addressed: Zhong Zheng, Tel: +1 310 206 5646; fax: +1 310 206 7783; zzheng@dentistry.ucla.edu.; Xinli Zhang, Tel: + 1 310 206 6546; fax: +1 310 206 7783; xinli@ucla.edu; Kang Ting, Tel: +1 310 206 6305; fax: +1 310 206 7783; kting@dentistry.ucla.edu.; Chia Soo, Tel: +1 310 794 5479; fax: +1 310 206 7783; bsoo@ucla.edu; Address: 675 Charles E Young Drive, South, MRL 2641, Los Angeles, CA 90095, USA.
[&]Chenshuang Li and Zhong Zheng contributed equally to this work.

Authors' contributions

CL, ZZ, and JJ conceived the study; CL, ZZ, WJ, and SL performed the *in vitro* and *in vivo* experiments, data interpretation, and statistical analysis, except that PH performed the animal injections; CL, ZZ, and PH conducted the gait scoring; ZM and XZ contributed to data interpretation; HP processed the videos; CL, ZZ, EAB, ECC, and XZ wrote and revised the manuscript; CTC provided original ENU-induced *Nell-1*-deficient mice; KT and CS provided the financial support; KT and CS supervised the entire study. All authors reviewed the final draft, and ZZ, XZ, KT, and CS approved the manuscript.

Availability of data and materials

The datasets supporting the conclusions of this article are included within the article and its supplementary information.

Abstract

Arthritis, an inflammatory condition that causes pain and cartilage destruction in joints, affects over 54.4 million people in the US alone. Here, for the first time, we demonstrated the emerging role of Neural EGFL like 1 (NELL-1) in arthritis pathogenesis by showing that *Nell-1*-haploinsufficient (*Nell-1$^{+/6R}$*) mice had accelerated and aggravated osteoarthritis progression with elevated inflammatory markers in both spontaneous primary osteoarthritis (OA) and chemical-induced secondary OA models. In the chemical-induced OA model, intra-articular injection of interleukin (IL)1β induced more severe inflammation and cartilage degradation in the knee joints of *Nell-1$^{+/6R}$* mice than in wildtype animals. Mechanistically, in addition to its pro-chondrogenic potency, NELL-1 also effectively suppressed the expression of inflammatory cytokines and their downstream cartilage catabolic enzymes by upregulating runt-related transcription factor (RUNX)1 in mouse and human articular cartilage chondrocytes. Notably, NELL-1 significantly reduced IL1b-stimulated inflammation and damage to articular cartilage *in vivo.* In particular, NELL-1 administration markedly reduced the symptoms of antalgic gait observed in IL1β-challenged *Nell-1$^{+/6R}$* mice. Therefore, NELL-1 is a promising pro-chondrogenic, anti-inflammatory dual-functional disease-modifying osteoarthritis drug (DMOAD) candidate for preventing and suppressing arthritis-related cartilage damage.

Keywords

Cartilage damage; Disease-modifying osteoarthritis drug (DMOAD); Inflammation; Neural EGFL like 1 (NELL-1); Osteoarthritis; Runt-related transcription factor 1 (RUNX1)

Introduction

Arthritis appears in over 100 identified diseases that can damage any joint in the body, causing inflammation that results in pain, stiffness, swelling, and decreased motion [1, 2]. As the leading cause of disability among adults, arthritis has been diagnosed in more than 10 million people in the United Kindom [1] and approximately 54.4 million people in the United States [2, 3]. In particular, osteoarthritis (OA) is the most common form of arthritis and affects around 18% of women and 10% of men over the age of 60 [4]. Unfortunately, the traditional use of analgesia [5] is insufficient for curative treatment since it does not reduce inflammation and cartilage damage [5–7]. Multiple adverse side-effects in the musculoskeletal, cardiovascular, and gastrointestinal systems [8–10] challenge the use of glucocorticoids as safe arthritis treatments, and nonsteroidal anti-inflammatory drugs (NSAIDs) reduce pain and inflammation in the short-term but do not effectively control arthritis progression [6]. Even more disappointing, the efficacy of disease-modifying antirheumatic drugs (DMARDs) that postpone rheumatoid arthritis (RA) progression by slowing or suppressing inflammation has not been replicated in OA clinical trials *via* systemic or local administration [11–13]. This likely occurs because these therapeutics do not directly manage cartilage destruction—the primary cause of OA [4, 6, 7, 14].

In order to combat the cartilage destruction seen in OA [4], the recent search for new OA therapeutics is shifting from synthetic chemicals to biological molecules, with a specific focus on pro-chondrogenic growth factors [7, 15–20]. For instance, neural EGFL-like 1

(NELL-1) is a novel pro-chondrogenic molecule that enhances the proliferation, chondrogenic differentiation, and maturation of chondrogenic-committed cells and their progenitors *in vitro* [21, 22]. As an extracellular matrix (ECM) molecule expressed in articular cartilage [21], NELL-1 alone is sufficient to promote cartilage regeneration without osteophyte formation in rabbit knee criticalsized, full-thickness subchondral defects [23]. Moreover, our recent studies identified a novel signaling cascade of NELL-1 → nuclear factor of activated T-cells (NFATc)1 → runt-related transcription factor (RUNX)3 → Indian hedgehog (IHH) in articular chondrocytes, which is essential for NELL-1's pro-chondrogenic bioactivities [22, 24, 25]. Inspired by the genome-wide association study (GWAS) that associated single nucleotide polymorphisms (SNPs) within the *NELL-1* gene with ankylosing spondylitis and psoriatic arthritis [26–28], the current study is intended to determine the role of NELL-1 in the pathogenesis of OA and its potential therapeutic benefits.

Materials and Methods

In silico prediction

In vitro half-life ($t_{1/2}$) and the time required for reduction to 10% of the original mature human NELL-1 protein content (t_{90}) in mammalian cells were predicted by the online server ProtParam (https://web.expasy.org/protparam/). The NELL-1 $t_{1/2}$ is approximately 1.1 h and the t_{90} is less than 6 h in mammalian cells *in vitro*. These predictions were further confirmed by ProtLifePred (http://protein-n-end-rule.leadhoster.com/).

Genomatix Software v3.10 (Genomatix AG, Munich, Germany) was used to predict the potential binding motifs of RUNX1 and NFATc1 in chondrocytes/cartilage. The sites were computationally projected with predefined transcriptional factor binding modules [29].

Human arthritic cartilage

Human arthritic cartilage samples were obtained from patients of both sexes between the ages of 32 and 92 undergoing knee arthroplasty with an institutional review board (IRB) exemption since no donor identities were provided for these samples. These pre-fixed samples were used for histological and immunobiological analyses only. Meanwhile, primary adult human articular chondrocytes (hARCs) isolated from normal/healthy (NM), OA, and RA donors were purchased from Cell Application Inc. (San Diego, CA, US) and cultured according to the manufacturer's instructions for *in vitro* investigations.

Animal maintenance

All the experiments on live mice were performed under an institutionally approved protocol provided by the Chancellor's Animal Research Committee at UCLA (protocol numbers: 2014-041 and 2013-013). Due to *N*-ethyl-*N*-nitrosourea (ENU)-induced homozygous *Nell-1*-deficient (*Nell-1^6R/6R*) mice having a severely reduced expression of *Nell-1* that results in neonatal death [30], *Nell-1*-haploinsufficient (*Nell-1^+/6R*) mice (a well-established loss-of-function model [22, 24, 25]) were examined in the current investigation. Mice were bred and maintained as previously described [22, 24, 25], and their genotypes were determined by polymerase chain reaction (PCR). Genetic knockdown of *Nell-1* was also

confirmed by immunofluorescence (IF) staining in the tibia cartilage of newborn *Nell-1*^{+/6R} mouse knees (Supplementary Fig. 1).

Primary osteoarthritis model

Slowly progressing OA in animals, such as in mice, closely simulates the natural progression of human primary OA [31]. Wild-type (WT) and *Nell-1*^{+/6R} mice at 1 month old (a prepubescent stage for mice that developmentally approximates 12.5 years of age in humans [32, 33]), 3-months-old (a young mature adult stage for mice that developmentally approximates 20 years of age in humans [33]), and 18-months-old (a senescent stage for mice that developmentally approximates >50 years of age in humans [33]) were used to understand Nell-1's activities in the pathogenesis of OA. Since the prevalence of OA in human is significantly higher in women than men [4], female mice were chosen for this proof-of-concept study. Special focus was directed to the medial tibial plateau area, which is one of the most critical loadbearing areas in the body [34]. The mice were euthanized with an overdose of phenobarbital (Piramal Healthcare, Maharashtra, India), and their right hind limbs were harvested for histological and IF staining. Expression levels of *Nell-1* in the medial tibial plateau cartilage were monitored using laser-capture microdissection (LCM)-coupled quantitative real-time PCR (Supplementary Fig. 2) as described below.

Secondary osteoarthritis model

An imbalance in chondrocyte functions, which can be induced by outside stimuli such as the presence of inflammatory cytokines, leads to the progression of degenerative conditions like OA. In particular, the local elevation of IL1β in rodent knee joints has been shown to induce OA-like symptoms [35–37]. Thus, a well-documented modified direct mouse intra-articular IL1β injection model [38] was used to simulate secondary OA-like damage *in vivo* [31]. Briefly, under isoflurane anesthesia (5% for anesthesia induction and 2% for maintenance), a Hamilton syringe with a 29-gauge needle was inserted through the patellar ligament into the joint space of the right knee of 2.5-month-old female WT or *Nell-1*^{+/6R} mice. Since the *in vivo* elimination $t_{1/2}$ of NELL-1 is 5.5 h [39], the intra-articular injection was performed twice daily by the same surgeon to avoid variation in technique. For each genotype, animals were randomly assigned to the four treatment groups (6 mice per group; Fig. 1) before the first injection: 'Control' group: 6 μl phosphate-buffered saline (PBS) per injection for 14 days; 'NELL-1' group: 6 μl PBS per injection for 7 days followed by 2 μg recombinant human NELL-1 (Aragen Bioscience, Inc., Morgan Hill, CA, US) in 6 μl PBS per injection for another 7 days; 'IL1β' group: 100 ng recombinant human IL1β (PeproTech, Inc., Rocky Hill, NJ, US) in 6 μl PBS per injection for 14 days; and 'IL1β + NELL-1' group: 100 ng IL1β in 6 μl PBS per injection for 7 days to trigger the inflammation, while 100 ng IL1β + 2 μg NELL-1 in 6 μl PBS per injection was administered for an additional 7 days. It is worth noting that, in the 'IL1β + NELL-1' group, IL1β was injected along with NELL-1 in the second 7 day injection period to avoid the influence of spontaneous cartilage recovery after withholding IL1β, which was previously observed [35, 40, 41], and to more accurately mimic the pathological OA condition in which inflammatory stimulation is persistent. For gait analyses, videos were captured on day 7 and 14 and evaluated independently by three experienced physicians in a blinded fashion before the animals were sacrificed for histological analysis. An established gait scoring system, which was previously used in an

inflammatory monoarthritic mouse model [42], was adapted to examine impacts on animal behavior (Supplementary Table 1) as recommended [43].

Histological and IF staining

The mouse hind limb and human arthritic cartilage samples were fixed in 4% paraformaldehyde (MilliporeSigma; Burlington, MA, US) at 4°C for 24 h and decalcified with 19% ethylenediaminetetraacetic acid (pH 8.0; MilliporeSigma) for 21 days prior to paraffin embedding and sectioning at a thickness of 5 μm. Hematoxylin and eosin (H&E) staining was performed for histological analysis, while safranin O staining was conducted with the NovaUltra™ Safranin O staining Kit (IHC World, LLC, Woodstock, MD, US) according to the manufacturer's instructions. Primary antibodies against type II collagen (N-N6B3, 1:20; Developmental Studies Hybridoma Bank, Iowa City, IA, US), IL1β (ab9722, 1:400; Abcam, Cambridge, MA, US), IL6 (TA500067, 1:50; Origene, Rockville, MD, US), matrix metallopeptidase (MMP)13 (ab39012, 1:200; Abcam), bone morphogenetic protein (BMP)6 (ab155963, 1:200; Abcam), BMP7 (ab84684, 1:1000; Abcam), RUNX1 (ab35962, 1:1000, Abcam), and NELL-1 (ABP-PAB-11648, 1:75; Allele Biotech, San Diego, CA, US) were used for IF staining. The Vector® M.O.M.™ Immunodetection Kit (Vector Laboratories, Inc., Burlingame, CA, US) was employed to locate mouse primary antibodies on mouse tissue. 4',6-diamidino-2-phenylindole (DAPI; MilliporeSigma) was used for nuclear counterstaining.

Laser-capture microdissection (LCM)

For LCM, fresh-cut tissue sections at 10 mm were mounted on polyethylene naphthalate (PEN) Membrane Glass Slides (2.0 μm, MicroDissect GmbH, Herborn, Germany). To visualize the medial tibial plateau area, tissue sections were stained with Cresyl Fast Violet and completely air dried before microdissection [44]. Tibial cartilage was microdissected on a Leica LMD7000 system (Leica, Buffalo Grove, IL, US). After microdissection, the excised region was examined microscopically (Supplementary Fig. 3) and was kept on ice until RNA isolation.

In vitro mechanism of action investigation

To gain initial insight into the mechanism underlying NELL-1's anti-arthritic bioactivities, primary articular cartilage chondrocytes were utilized for the *in vitro* investigation because: (1) chondrocytes are primary contributors to articular cartilage structural support, metabolic activities, and critical maintenance functions, such as ECM secretion, within joints [45]; (2) chondrocytes are a confirmed cell source that secretes NELL-1 [21, 22, 24, 25]; (3) local secretion of proinflammatory cytokines, including IL1β, IL6, and tumor necrosis factor (TNF)α [46–49] by articular chondrocytes can activate their autocrine loops, which are essential for the initiation and progression of arthritis [50–53]; and (4) the regulatory roles of these proinflammatory cytokines are at least partially independent from those of synovial and immune cells [53]. In particular, previous studies have confirmed that proinflammatory cytokines, including IL1β, can induce arthritis-like biological changes in articular chondrocytes *in vitro* [53]. Expression of proinflammatory cytokines IL1β, IL6, and TNFα, their downstream catabolic markers MMP13 and ADAM metallopeptidase with thrombospondin type 1 motif (ADAMTS)5, which are major contributors to ECM

degradation during arthritis progression [54, 55], the chondrocyte-secreted inflammatory maker prostaglandin-endoperoxide synthase (PTGS)2 [53], and the anabolic marker type II collagen (encoded by *COL2α1*) were evaluated. Based on aforementioned *in silico* predictions, all assessments were conducted in the 6 h post-treatment window since the t_{90} of NELL-1 was estimated to be less than 6 h in mammalian cells.

Primary mouse articular chondrocyte isolation and cultivation

Primary mouse articular cartilage chondrocytes (mARCs) were isolated and cultivated as previously described [56–58]. Briefly, small pieces of articular cartilage, located at distant sites from the synovial tissue, were removed from 3-month-old female WT or *Nell-1*$^{+/6R}$ mice. These cartilage tissues were digested in 1.5 mg/ml collagenase B (MilliporeSigma) at 37°C overnight to achieve single-cell suspensions. After rinsing with Dulbecco's Modified Eagle's Medium (DMEM), mARCs were cultured in a basal culture medium [DMEM with 10% fetal bovine serum (FBS), 100 U/ml penicillin, and 100 μg/ml streptomycin]. The medium was changed every 3 days, and the cells were passaged at 70~90% confluence. All of these cell culture reagents were purchased from Thermo Fisher Scientific (Canoga Park, CA, US).

Gene expression analysis

Chondrogenic-committed ATDC5 cells were obtained from the RIKEN Cell Bank (Tsukuba, Japan) and cultured in DMEM/Ham's F-12 medium (Thermo Fisher Scientific) containing 5% FBS. Passage 2 primary mARCs, isolated from 3-month-old female WT and *Nell-1*$^{+/6R}$ mice, and commercially available primary hARCs were also used for gene expression analysis. Subconfluent cells were subjected to serum starvation (0.1% FBS) for 18 h and stimulated with 10 ng/ml recombinant human IL1α with or without 0.8 or 2.0 μg/ml recombinant human NELL-1.

Total RNA isolated by the RNeasy® Mini Kit (for ATDC5 cell, mARCs, or hARCs; Qiagen, Germantown, MD, US) or the RNeasy® FFPE Kit (for mouse cartilage samples obtained by LCM; Qiagen) with DNase treatment was used for reverse transcription with the iScript™ Reverse Transcription Supermix for RT-qPCR (Bio-Rad Laboratories Inc., Hercules, CA, US). In particular, tibial cartilage samples collected from two animals were pooled together for RNA isolation to obtain enough RNA for analysis. One μl of reverse transcription product was used for real-time PCR with SsoAdvanced™ Universals Probes Supermix (Bio-Rad Laboratories Inc.) and TaqMan® primers/probe sets (Supplementary Table 2; Thermo Fisher Scientific) on a QuantStudio3 system (Thermo Fisher Scientific). For each individual real-time PCR assay, three independent reserve transcription reaction products were used as templates and tested in duplicate.

Enzyme-linked immunosorbent assay (ELISA)

The mouse IL-6 Platinum ELISA Kit (Cat. # BMS603–2), mouse TNF alpha Uncoated ELISA Kit (Cat. # 88–7324), human IL-6 ELISA Kit (Cat. # BMS213–2), human TNF alpha Uncoated ELISA Kit (Cat. # 88–7346), and human MMP-13 ELISA Kit (Cat. # EHMMP13) were purchased from Thermo Fisher Scientific, while the mouse Mmp13 ELISA Kit was purchased from MyBioSource.com (Cat. # MBS2884671; San Diego, CA,

US). Five x 10^4 cell/well in 24-well plates were treated with 1 ml medium. Cell culture medium was collected 6 h post-treatment for ELISA analyses according to the manufacturers' instructions.

Reduced representation bisulfite sequencing (RRBS)

RRBS was conducted by the Technology Center for Genomics & Bioinformatics at UCLA. Briefly, gDNA was extracted from NM-, OA-, and RA-hARCs using the AllPrep DNA/RNA/Protein Mini Kit (Qiagen). Library preparation began by using the Nextflex® Bisulfite-Seq Library Prep Kit followed by a *MspI* restriction enzyme digestion (PerkinElmer, Waltham, MA, US). First, digestion was performed, end-repair and ligation of Met-Seq adapters followed, and size selection occurred subsequently. Bisulfite conversion was performed using the EZ DNA Methylation-Gold Kit (Zymo Research, Irvine, CA, US). The subsequent step consisted of PCR amplification for 17 cycles. This library was sequenced on a 150 bp, pair-end, HiSeq 3000 (Illumina, San Diego, CA, US) sequencing run. Data quality checks were performed on the *Illumina SAV*. Demultiplexing was performed with the *Illumina Bcl2fastq2 v2.17 program*. Sequencing data were aligned to the GRCh37 (hg19) genome *via Bismark* [59]. Alignment was quantified and translated to total CpG count using *Bismark*'s *Methylation Extractor* module. More than 90% of the reads were aligned to the genome (Supplementary Table 3), which was in the standard range for RRBS. Differential methylation was performed using *diffmeth* and annotation was performed with *identgeneloc,* which are modules that are included in the *DMAP* package [60].

RNA interference (RNAi)

Plasmid packages harboring shRNA that targeted mouse *Runx1* (G151145_0-3) and *Nfatc1* (TG5010315_A-D), respectively, were purchased from OriGene (Rockville, MD, USA) and used to create stable ATDC5 knockdown cell lines with 4 μg/ml puromycin (Thermo Fisher Scientific) following the 'Application Guide' provided by the vendor. A scramble control vector (TR30013) provided by OriGene was also used to establish a stable control ATDC5 cell line.

Statistics

All statistical analyses were conducted in consultation with the UCLA Statistical Biomathematical Consulting Clinic. The sample size for each individual experiment is presented in the respective figure legends. For the gene expression and ELISA assays, one-way ANOVA and two-sample *t*-test analyses were performed by OriginPro 8 (Origin Lab Corp., Northampton, MA, USA), while the Kruskal-Wallis ANOVA, Mann-Whitney *U* test, or paired-sample Wilcoxon test were used to analyze gait scoring. For all data presented in this manuscript, $P < 0.05$ (*) was considered a suggestive difference, while $P < 0.005$ (**) was recognized as a statistically significant difference based on a recent recommendation [61].

Results

Nell-1-haploinsufficiency is prone to arthritis-like pathologic changes with increased proinflammatory cytokines in mouse knee articular cartilage.

Similar to humans, mice naturally develop OA during maturation, which qualifies them as a primary OA model to study inflammation in joints [31]. At 1 month old, there were no apparent differences in cartilage degeneration or inflammation between the knees of WT and *Nell-1*$^{+/6R}$ mice (Supplementary Figs. 4 and 5) except that *Nell-1*$^{+/6R}$ tibial cartilage chondrocytes had slightly reduced *Col2a1* expression accompanied by increased *Il6* transcription (Supplementary Fig. 5B and D). Pathologically, the thicknesses of the entire articular cartilage were similar in both WT and *Nell-1*$^{+/6R}$ mice. However, unlike WT mice whose uncalcified hyaline cartilage (HC) above the tidemark constituted the major portion of the cartilage, *Nell-1*$^{+/6R}$ mice had cartilage in which the superficial HC and underlying calcified cartilage (CC) layer below the tidemark presented similar thicknesses, indicating that CC already expanded during the early adolescence period of *Nell-1*$^{+/6R}$ mice [32].

At 3 months of age, focal wear and tear of HC with early chondrocyte clustering were only observed in *Nell-1*$^{+/6R}$ mice, accompanied by a lower HC/CC ratio than in age-matched WT counterparts (Fig. 2A). In comparison with WT cartilage, *Nell-1*$^{+/6R}$ cartilage not only had significant type II collagen reduction and Mmp13 elevation at both the protein and RNA levels that represent key events in OA progression [54], but also had remarkedly pronounced Il1β and Il6 expression, which indicates elevated inflammation (Fig. 2A and Supplementary Fig. 5).

At 18 months of age, limited wear and tear was found in HC layer of WT cartilage with decreased type II collagen and increased Mmp13 and Il1β (Fig. 2B); a profile that exhibited great similarity to that of 3-month-old *Nell-1*$^{+/6R}$ mice. In contrast, severe loss of HC [containing almost completely absent proteoglycan, negligible type II collagen, but significantly upregulated Mmp13, Il1β, and Il6 (Fig. 2B and Supplementary Fig. 5)] and exposure of the underlying CC were observed in 18-month-old *Nell-1*$^{+/6R}$ mouse knees. These histological and immunological changes were similar to those seen in late-stage OA of human patients [62].

Taken together, encompassing the age spectrum from juvenile, young adult, to elderly, *Nell1*-haploinsufficiency drastically accelerated and aggravated the arthritis-like cartilage degeneration in mice and was accompanied with significant elevation of proinflammatory cytokines.

Intra-articular injection of IL1β induced exaggerated OA-like damage in *Nell-1*$^{+/6R}$ mouse knees.

As a secondary OA model [31], 7 days of intra-articular IL1β injection (Fig. 1) was sufficient to induce proteoglycan degradation and upregulate proinflammatory cytokines Il1β and Il6 in HC of articular cartilage of 2.5-month-old WT mice (Supplementary Fig. 6). Continuously challenging the joints with IL1β for 14 days led to more severe arthritis-like damage, as characterized by (1) complete abolishment of proteoglycan expression on the tibial and femoral cartilage, (2) minimal staining of type II collagen on both HC and CC, (3)

increased expression of Mmp13 in HC, and a significant boost in Il1β and Il6 levels in HC (Fig. 3A: 'IL1β', and Supplementary Fig. 7A–D). However, this damage was not severe enough to significantly alter the mobility of WT mice (Supplementary Fig. 8A). In comparison with age-matched WT counterparts, IL1β injection for 7 days in 2.5-month-old *Nell-1*[+/6R] mouse knees resulted in a more advanced decrease of proteoglycan and type II collagen, as well as bursts of increased Mmp13, Il1β, and Il6 levels (Supplementary Fig. 6). More importantly, 14 days of IL1β injection in 2.5-month old *Nell-1*[+/6R] mice (3 months old at the end of treatment) replicated the drastic arthritis-like damage seen in 18-month old *Nell-1*[+/6R] mice with regard to HC erosion, proteoglycan degradation, and Mmp13 expression, in addition to even more severely reduced type II collagen and increased inflammation (Fig. 3B: 'IL1β', and Supplementary Fig. 7A–D). In congruence with the histological assessment, the symptoms of antalgic gait were observed among 'IL1β' group *Nell-1*[+/6R] mice (Supplementary Video 1: 'IL1β', and Supplementary Fig. 8B). Therefore, IL1β induced more severe arthritis-like damage in *Nell-1*[+/6R] mouse knees.

NELL-1 injection rescued IL1β-induced arthritis-like damage in adult mouse knees.

To estimate the potential therapeutic benefits of NELL-1 against arthritic damage, NELL-1 was administered in the aforementioned intra-articular injection model with or without an accompanying IL1β challenge (Fig. 1). In WT mice, in comparison with a PBS vehicle control (Fig. 3A: 'Control'), NELL-1 injections alone slightly increased the amount of proteoglycan and type II collagen with less Il1β staining in HC (Fig. 3A: 'NELL-1'). In *Nell-1*[+/6R] mice, NELL-1 alone upregulated proteoglycan and type II collagen deposition in knee cartilage, while simultaneously reducing the expression of Il1β and Il6 to comparable levels of those in the age-matched WT animals (Fig. 3B: 'NELL-1', and Supplementary Fig. 7).

When NELL-1 was administered with IL1β after the initial 7 days of IL1β-challenging, the IL1β-induced arthritis-like damage was partially rescued in WT animals, as detected by the presence of safranin O staining, upregulation of type II collagen density, and observation of IL1β and Il6 signals similar to those of the 'Control' group (Fig. 3A: 'IL1β + NELL-1', and Supplementary Fig. 7). Similarly, administration of exogenous NELL-1 significantly reduced the inflammatory response and damage to articular cartilage in IL1β-challenged *Nell-1*[+/6R] mice (Fig. 3B: 'IL1β + NELL-1'. and Supplementary Fig. 7). Importantly, the symptoms of antalgic gait in 'IL1β + NELL-1' treated *Nell-1*[+/6R] mice were moderate, and far less severe than the symptoms observed in 'IL1β' group *Nell-1*[+/6R] animals (Supplementary Video 1: 'IL1β + NELL-1', and Supplementary Fig. 8B). Excitingly, in a second validation experiment that tracked the mobility of 'IL1β + NELL-1' group *Nell-1*[+/6R] animals, the antalgic gait driven by the 7-day IL1β-challenge was drastically reduced by the subsequent 7 days of exogenous NELL-1 and IL1β administration in all 6 tested *Nell-1*[+/6R] mice (Supplementary Videos 2–7 and Supplementary Fig. 8C). Collectively, our present data demonstrate that NELL-1 has possible therapeutic potential for preventing and controlling the pathogenesis of arthritis.

NELL-1 significantly reduced IL1β-stimulated expression of inflammatory and catabolic molecules in mouse and human articular chondrocytes *in vitro*.

In alignment with the aforementioned mouse models in which low Nell-1 levels correlated with high inflammation and *vice versa,* we observed that intense IL1β staining was generally accompanied by low levels of NELL-1, but was not necessarily associated with less BMP6 or BMP7, in human arthritic articular cartilage lesions (Supplementary Fig. 9). This observation encouraged us to hypothesize that, in addition to its pro-chondrogenic functions, NELL-1 may also directly reduce inflammation in both mouse and human arthritis.

As expected, *Nell-1*-haploinsufficiency led to increased expression of proinflammatory and catabolic genes in primary mARCs (Fig. 4A–F). On the other hand, an apparent NELL-1 dose-dependent decline in proinflammatory and catabolic gene expression was generally observed when the mARCs were treated with NELL-1 protein alone (Fig. 4A1–F2). Meanwhile, IL1β significantly induced the transcription of all tested proinflammatory and downstream catabolic markers in both WT- and *Nell-1$^{+/6R}$-mARCs,* which were consistently blocked by NELL-1 (Fig. 4A1–F2). The anti-inflammatory effects of NELL-1 on mARCs were further confirmed at the protein levels using ELISA (Supplementary Fig. 10). In comparison with WT-mARCs, *Nell-1$^{+/6R}$*-mARCs also had lower levels of *Col2a1* (which encodes the anabolic maker type II collagen; Fig. 4G), which further supports the pro-chondrogenic role of NELL-1. IL1β also markedly reduced *Col2a1* expression in both WT- and *Nell-1$^{+/6R}$-mARCs,* and its effects were seemingly more pronounced in *Nell-1$^{+/6R}$-mARCs* (Fig. 4G1–G2), while a higher dose (2 μg/ml) of NELL-1 completely eliminated the downregulation of *Col2a1* caused by IL1β-stimulation or *Nell-1*-haploinsufficiency (Fig. 4G1–G2). Interestingly, we also noticed that NELL-1 administration upregulated endogenous *Nell-1* expression in mARCs (Fig. 4H–H2), which is in agreement with the results from the *in vivo* studies (Supplemental Fig. 7E). Taken together, these data reveal that NELL-1 could, at least partially, rescue mARCs from invoking chondrogenic ECM degradation and inflammation induced by endogenous *Nell-1*-deficiency or exogenous IL1β-stimulation.

Furthermore, the aforementioned bioactivities of NELL-1 were also validated in primary hARCs isolated from NM, OA, and RA donors. In comparison with NM-hARCs, OA- and RA-hARCs had elevated levels of proinflammatory and catabolic markers, which were generally downregulated by exogenous NELL-1 application (Fig. 5A–F3). Due to the well-documented species-specific activity among mammalian IL1β [63, 64], hARCs, in comparison with mARCs, demonstrated a greater increase in proinflammatory and catabolic gene expression in response to recombinant human IL1β administration. Further, as expected, NELL-1 actively reduced the IL1μ-stimulated inflammatory responses in hARCs (Fig. 5A1–F3 and Supplementary Fig. 11). Collectively, our current data indicate that, as a pro-chondrogenic agent, NELL-1 also has a protective function against inflammation in chondrocytes, and thus, has the potential to be used as a disease-modifying osteoarthritis drug (DMOAD).

Additionally, less *COL2a1* was expressed by OA- and RA-hARCs in comparison with NM-hARCs; *COL2a1* transcription was reduced by IL1β and increased by NELL-1 in hARCs, which was similar to the effects of IL1β and NELL-1 seen in mARCs (Fig. 5G–G3).

Meanwhile, OA- and RA-hARCs have significantly lower levels of *NELL-1* than NM-hARCs (Fig. 5H), while RA-hARCs also exhibited higher CpG methylation levels at the NELL-1 locus than NM-hARCs (Supplementary Table 4), suggesting NELL-1 may also be involved in the pathogenesis of RA.

RUNX1 mediates NELL-1's anti-inflammatory activities.

Previous studies demonstrate that *NFATc1* and *RUNX1* are primary genes that respond to NELL-1 in chondrocytes [25]. An *in silico* bioinformatic prediction indicates that both NFATc1 and RUNX1 potentially bind to promoters of *IL1β* and/or *TNFα* in human and mouse cartilage/chondrocytes (Supplementary Table 5). Since the anti-inflammatory effects of NELL-1 on primary mARCs and hARCs were replicated in ATDC5 cells (Supplementary Fig. 12), RNAi was used to establish stable *Nfatc1-* and *Runx1*-knockdown (KD) ATDC5 cells, respectively (Supplementary Fig. 13), to examine whether RUNX1 and/or NFATc1 mediate NELL-1's anti-inflammatory activities in chondrocytes. In agreement with previous observations that both RUNX1 and NFATc1 are negative regulators of inflammation in arthritic conditions [65–68], *Nfatc1-* and Runx1-KD ATDC5 cells had higher endogenous levels of *Il1β, Il6,* and *Tnfα* (Fig. 6A–C). Moreover, IL1β administration induced more pronounced elevation of these proinflammatory genes in *Nfatc1-* and *Runx1*-KD ATDC5 cells than in the scramble control plasmid transfected (scramble) ATDC5 cells (Fig. 6A1–C3).

NELL-1's anti-inflammatory effects were conserved in the *Nfatc1*-KD ATDC5 cells (Fig. 6A2–C2) at the same level as in the scramble ATDC5 cells (Fig. 6A1–C1). On the contrary, Runx1-KD almost completely eliminated NELL-1's anti-inflammatory bioactivity in ATDC5 cells (Fig. 6A3–C3 and Supplementary Fig. 14). Interestingly, in comparison with non-transfected or scramble ATDC5 cells, although *Runx1* upregulation was largely reduced and postponed in *Runx1*-KD ATDC5 cells (Supplementary Fig. 15), the leaking *Runx1* elevation induced by a high dose (2 μg/ml) of NELL-1 at 6 h post-treatment was still sufficient to markedly weaken the IL1β-responsive expression of *Il1β* in *Runx1*-KD ATDC5 cells (Fig. 6A3). This phenomenon further supports the hypothesis that RUNX1 is essential and adequate to render NELL-1's anti-inflammatory activity in chondrocytes. We also observed that *Nell-1^{+/6R}* mARCs had decreased *Runx1* expression (Supplementary Fig. 16A), while OA- and RA-hARCs had lower *RUNX1* levels in comparison with NM-hARCs (Supplementary Fig. 17A). Moreover, NELL-1 significantly upregulated *Runx1/RUNX1* in all tested primary mARCs and hARCs *in vitro* (Supplementary Fig. 16B–C and Supplementary Fig. 17B–D). This gene expression alteration has been further confirmed at the protein level in the aforementioned intra-articular injection model *in vivo*: intra-articular NELL-1 administration upregulated Runx1 protein in mouse knee cartilage, which was not altered by the absence or presence of IL1β-stimulation or by *Nell-1*-haploinsufficiency alone (Fig. 7 and Supplementary Fig. 7F). Taken together, these data suggest that RUNX1, instead of NFATc1, is a key downstream mediator of NELL-1's anti-inflammatory bioactivity in chondrocytes (Fig. 8).

Discussion

An ideal OA-combating agent that has the ability to safely reduce inflammation and promote cartilage regeneration has long been desired. The traditional use of analgesia is insufficient for curative treatment since it does not reduce inflammation and cartilage damage [5–7]; multiple adverse side-effects in the musculoskeletal, cardiovascular, and gastrointestinal systems [8, 9] challenge the use of glucocorticoids as safe arthritis treatments, and NSAIDs do not effectively control arthritis progression [6]. Even more disappointing, the efficacy of DMARDs that postpone RA progression by slowing or suppressing inflammation has not been replicated in OA clinical trials *via* systemic or local administration [11–13]. This likely occurs because these therapeutics do not directly manage cartilage destruction – the primary cause of OA [4, 5]. At this time, the prospect of using well-known pro-chondrogenic growth factors as treatments for arthritis does not appear to be optimistic either. For instance, administration of BMP7 can downregulate multiple cartilage catabolic molecules in OA-damaged tissue, but it does not notably alter proinflammatory cytokine expression [18]. Intra-articular injection of transforming growth factor (TGF)β even appears to further elevate inflammatory infiltration in treated joints [15, 16], while BMP6 can induce the production of proinflammatory cytokines, such as TNFα [19], from macrophages – a major cell type responsible for inflammation and destruction in OA-ridden synovium [17].

In addition to our recent studies that revealed and confirmed the important regulatory roles of NELL-1 in chondrogenic development and maturation [21–25], we also noticed a negative correlation between proinflammatory markers and NELL-1 in both mouse and human arthritic articular cartilage. Specifically, by using spontaneous primary OA and chemical-induced secondary OA models, we further demonstrated that *Nell-1*-deficiency could accelerate and aggravate the progression of OA. Meanwhile, we documented a correlative decrease in *NELL-1* expression with higher levels of proinflammatory cytokines found in OA-hARCs than NM-hARCs. To the best of our knowledge, this is the first time the emerging role of NELL-1 in arthritis pathogenesis has been elucidated.

Furthermore, RA-hARCs exhibited higher CpG methylation at the NELL-1 locus and lower *NELL-1* transcription than NM-hARCs, which is in accordance with a previous microarray investigation that detected reduced *NELL-1* expression in the damaged knee cartilage of anteromedial gonarthrosis patients [69]. In addition, SNPs within the *NELL-1* gene have been detected in patients diagnosed with ankylosing spondylitis and psoriatic arthritis [26–28]. These phenomena indicate that NELL-1 may also be closely connected to the progression of a broad range of arthritis conditions; however, this observation should be further verified with a large number of arthritis patients. Moreover, determining whether alterations of *NELL-1's* genetic, epigenomic, and transcriptional levels are consequences or causes of continuous inflammatory infiltration should be carefully delineated in the future.

With NELL-1-stimulated chondrogenic regeneration observed in articular cartilage defects *in vivo,* there is an expected benefit of NELL-1 when used as arthritis therapeutic [23]. For example, when healthy, CC remains relatively constant in articular cartilage since the chondrocytes within CC typically stay quiescent during adulthood [70]. In this study, we found that intra-articular NELL-1 injection led to a moderately thickened CC layer of the

tibial plateau cartilage in both WT and *Nell-1*[+/6R] mice. Importantly, unlike CC reactivation in OA as a result of progressive calcification of the unmineralized cartilage that reduces the thickness of HC and the entire articular cartilage [70], NELL-1-induced CC expansion was not accompanied by noticeable HC reduction. Since recent studies revealed that articular cartilage contains mesenchymal stem cells (MSCs) and/or chondroprogenitors that are most abundant in, but not limited to, the superficial zone [71], NELL-1-induced CC expansion may result from its ability to stimulate the proliferation and chondrogenic differentiation of MSCs and chondroprogenitors [21], representing a wave of chondrogenesis in adult animals. In addition to its observed pro-chondrogenic effects, NELL-1 is able to downregulate the expression of proinflammatory and catabolic molecules, and as a result, demonstrate an anti-inflammatory potency *in vitro* and *in vivo*. Importantly, our current data demonstrate the potential of NELL-1 to rescue severe cartilage damage and reduce the symptoms of antalgic gait in an IL1β-challenged animal model that simulates OA pathogenesis, which could be attributed to NELL-1's pro-chondrogenic and anti-inflammatory dual-potency (Fig. 8). Encouragingly, previous studies have not revealed any noticeable adverse effects when NELL-1 was investigated and used for treating osteoporosis, even with systemic delivery and chemical modification that dramatically prolongs its elimination $t_{1/2}$ and distribution in the musculoskeletal system [39, 72]. Therefore, from both efficacy and safety standpoints, NELL-1 shows potential as a novel and promising DMOAD candidate in response to the unmet demand for OA therapeutics [20].

Until now, NFATc1 and NFATc2 are the most studied NELL-1 downstream effectors for chondrogenesis. Both NFATc1 and NFATc2 have been found to play important roles in maintaining cartilage health and repressing spontaneous OA [67, 68]. In particular, *Nfatc2*^{−/−} mice develop OA between 12 to 24 months of age [73, 74], which is even more markedly accelerated by cartilage-specific ablation of *Nfatc1* [67]. Despite this, the current understanding of the NFATc proteins' actions in arthritis is unclear due to the controversial data. For instance, inhibition of calcineurin, an NFATc activator, decreased the severity of OA [75], while blocking glycogen synthase kinase 3β, an NFATc inhibitor, induced OA in mice [76]. Further, IL1β was found to induce the expression of *NFATc1* in hARCs [77]. These observations differ from previously reported anti-arthritic effects of NFATc molecules [67, 68, 74]. By demonstrating that NFATc1 plays an essential role in mediating NELL-1's pro-chondrogenic bioactivities *via* activation of the IHH signaling pathway [22, 24, 25], but that it is not a prerequisite for NELL-1's anti-inflammatory potency (Fig. 8), our studies provide unique insight into determining the intricate roles of NFATc1 in arthritis, which may reconcile these seemly conflicting observations.

RUNX1 is another arthritis susceptibility gene [78–80] that has been targeted for DMOAD development [65, 81, 82]. Aini *et al.* demonstrated that intra-articular injection of *RUNX1* mRNA resulted in upregulated anabolic gene expression accompanied by lower Il1β levels in OA mouse articular cartilage [66]. Following our previous studies that identified *RUNX1* as a NELL-1-responsive gene in chondrocytes [25], this study demonstrates that RUNX1 is a key negative inflammatory regulator mobilized by NELL-1 and plays an anti-inflammatory protective role in the development of OA (Fig. 8). To our knowledge, this is the first time in which a functional upstream activator of RUNX1 has been identified for its therapeutic potency in chondrocytes.

Nevertheless, the understanding of the NELL-1 → RUNX1 –I IL1β functional axis is incomplete. First, the signal transduction from NELL-1 to RUNX1 is largely unknown, which may be partly due to the limited knowledge of NELL-1's specific cell surface receptor(s), associated protein(s), and downstream activators. NELL-1 may provide its function through different cell surface receptor(s) or co-receptor(s) in a cell-type- and develop-stage-dependent manner [83]. Meanwhile, the detailed mechanism of RUNX1 in arthritis is not yet clear [84, 85]. Moreover, we noticed that, although IL1β did not necessarily alter articular cartilage chondrocyte *NELL-1* expression in the short timeframe after exposure, the presence of IL1β profoundly blocked endogenous *NELL-1* upregulation that was expected in response to exogenous NELL-1 stimulation (Figs. 4H1–H2 and 5H1–H3). Given these facts, the interactions among NELL-1, RUNX1, and IL1β are far more complicated than they initially appear. Additionally, the mechanism behind the critical anti-arthritic autoinduction-like effect of NELL-1 *in vitro* (Figs. 4H1–H2 and 5H1–5H3) and *in vivo* (Supplementary Fig. 7E) is an interesting topic for subsequent investigation. Furthermore, the effects of NELL-1 on synovial and immune cells in the vicinity should also be assessed to fully elucidate the benefits of NELL-1 in arthritis management.

There appears to be no animal model used as the gold standard for osteoarthritis [86]. In the current study, a naturally occurring OA model gave the best representation of human primary OA and a chemical-induced model simulated human secondary OA to demonstrate the importance and potential therapeutical application of NELL-1 as a DMOAD. Chemical-induced OA models (such as the intra-articular IL1β injection model used in this study) are preferred for elucidating the genetic and molecular pathogenesis and identifying targets for drug therapy since they have no correlation to post-traumatic OA [31]. However, from a clinical aspect, the anti-arthritic efficacy of NELL-1 should be further confirmed in a post-traumatic OA model since both the tested models in this study do not simulate post-traumatic OA, which constitutes 12% of all symptomatic OA cases [87]. For instance, the surgical anterior (cranial) cruciate ligament transection (ACLT) model is the earliest and the most commonly used surgical model for simulating post-traumatic OA [31, 86]. Meanwhile, in comparison with small animals such as mice and rats, large animals have more anatomical and biomechanical similarities to humans [31,86]. In particular, goat knees have the closest anatomical resemblance to human knees [88]. Thus, a goat ACLT model may be useful for validating NELL-1's anti-arthritic potency and provide more clinically relevant data. The occurrence of OA is significantly higher in women [4, 31], which prompted the use of female animals in our current proof-in-concept study. However, the effect of gender and reproductive status should also be evaluated in future translational studies. Lastly, the repeat intra-articular injection strategy that was used in this study is clearly not the optimal administration route for clinical treatment. Further optimization with regard to the dose and treatment regimen of NELL-1 administration should be conducted before NELL-1 can be used in clinical applications. Previous studies revealed that the *in vivo* elimination $t_{1/2}$ of NELL-1 is only 5.5 h [39]; therefore, developing a suitable delivery vehicle and/or chemical modifications (such as PEGylation [39]) may also be needed to protect NELL-1 from endogenous enzyme digestion and subsequently elongate its biopotency *in vivo*. Taken together, considering that the investigation of NELL-1 in arthritis is in its infancy, a broad-

range collaboration among academic, clinical, and therapeutic researchers is essential for facilitating the bench-to-bedside translation of this potential treatment.

Conclusions

In summary, by using a loss-of-function *Nell-1*^{+/6R} mouse model, we demonstrated that NELL-1 has an anti-inflammatory role to protect articular cartilage from aggravated OA progression in addition to its previously exhibited pro-chondrogenic effects. Moreover, intra-articular injection of IL1β induced more severe inflammation and cartilage degradation in the knee joints of *Nell-1*^{+/6R} mice than in WT control animals, while administration of exogenous NELL-1, used as a gain-of-function model, significantly reduced the inflammatory response and articular cartilage damage in both WT and *Nell-1*^{+/6R} mouse knees. Excitingly, the heavy antalgic gait observed in IL1β-challenged *Nell-1*^{+/6R} mice notably recovered after NELL-1 administration. The anti-inflammatory effects of NELL-1 were also replicated *in vitro*, as evidenced by strong repression of IL1β–stimulated inflammatory markers and their downstream catabolic enzymes that are responsible for cartilage ECM degradation. By taking advantage of RNAi technology, we demonstrate that RUNX1, instead of NFATc1, mediates the anti-inflammatory activities of NELL-1 in chondrocytes. Collectively, for the first time, our current study not only demonstrates the emerging role of NELL-1 in arthritis pathogenesis but also introduces NELL-1 as a promising new-generation DMOAD for preventing and suppressing arthritis-related cartilage damage on account of its pro-chondrogenic and anti-inflammatory potency, both of which are absent in currently available OA medications. Future investigation is strongly encouraged to uncover the detailed underlying mechanism and optimize the dose, regimen, and delivery method for transferring NELL-1-based therapies into clinical practice.

Supplementary Material

Refer to Web version on PubMed Central for supplementary material.

Acknowledgments

References

[1]. Arthritis. NHS of UK Available from: https://www.nhs.uk/conditions/arthritis/.

[2]. Arthritis types. CDC of US Available from: https://www.cdc.gov/arthritis/basics/types.html.

[3]. Understanding arthritis. Arthritis Foundation Available from: https://www.arthritis.org/about-arthritis/understanding-arthritis/.

[4]. International ORS. Osteoarthritis: A serious disease. Osteoarthritis Research Society International 2016 p. 1–103.

[5]. Appleton CT. Osteoarthritis year in review 2017: Biology. Osteoarthritis And Cartilage. 2018;26:296–303. [PubMed: 29061493]

[6]. Scott DL. Arthritis in the elderly In: Fillit HM, Rockwood K, Woodhouse K, editors. Brocklehurst's textbook of geriatric medicine and gerontology. 7th ed. Philadelphia: SAUNDERS, ELSEVIER; 2010 p. 566–576.

[7]. Li C, Zou M, Zheng Z. Current medication for osteoarthritis. Acta Scientific Orthopaedics. 2018;1:09–12.

[8]. Cooper C, Bardin T, Brandi ML, Cacoub P, Caminis J, Civitelli R, et al. Balancing benefits and risks of glucocorticoids in rheumatic diseases and other inflammatory joint disorders: New insights from emerging data. An expert consensus paper from the European society for clinical and economic aspects of osteoporosis and osteoarthritis (ESCEO). Aging Clinical And Experimental Research. 2016;28:1–16. [PubMed: 26746234]

[9]. Compston J Glucocorticoid-induced osteoporosis: An update. Endocrine. 2018;61:7–16. [PubMed: 29691807]

[10]. Habib GS, Saliba W, Nashashibi M. Local effects of intra-articular corticosteroids. Clinical Rheumatology. 2010;29:347–356. [PubMed: 20101428]

[11]. Verbruggen G, Wittoek R, Cruyssen BV, Elewaut D. Tumour necrosis factor blockade for the treatment of erosive osteoarthritis of the interphalangeal finger joints: A double blind, randomised trial on structure modification. Annals of the Rheumatic Diseases. 2012;71:891–898. [PubMed: 22128078]

[12]. Chevalier X, Ravaud P, Maheu E, Baron G, Rialland A, Vergnaud P, et al. Adalimumab in patients with hand osteoarthritis refractory to analgesics and nsaids: A randomised, multicentre, double-blind, placebo-controlled trial. Annals of the Rheumatic Diseases. 2015;74:1697–1705. [PubMed: 24817417]

[13]. Chevalier X, Goupille P, Beaulieu AD, Burch FX, Bensen WG, Conrozier T, et al. Intraarticular injection of anakinra in osteoarthritis of the knee: A multicenter, randomized, double-blind, placebo-controlled study. Arthritis & Rheumatism-Arthritis Care & Research. 2009;61:344–352. [PubMed: 19248129]

[14]. van Laar M, Pergolizzi JV Jr., Mellinghoff HU, Merchante IM, Nalamachu S, O'Brien J, et al. Pain treatment in arthritis-related pain: Beyond nsaids. The Open Rheumatology Journal. 2012;6:320–330. [PubMed: 23264838]

[15]. Allen JB, Manthey CL, Hand AR, Ohura K, Ellingsworth L, Wahl SM. Rapid onset synovial inflammation and hyperplasia induced by transforming growth factor beta. The Journal of Experimental Medicine. 1990;171:231–247. [PubMed: 2295877]

[16]. Fava RA, Olsen NJ, Postlethwaite AE, Broadley KN, Davidson JM, Nanney LB, et al. Transforming growth factor beta 1 (TGF-beta 1) induced neutrophil recruitment to synovial tissues: Implications for TGF-beta-driven synovial inflammation and hyperplasia. The Journal of Experimental Medicine. 1991;173:1121–1132. [PubMed: 2022923]

[17]. Bondeson J, Wainwright SD, Lauder S, Amos N, Hughes CE. The role of synovial macrophages and macrophage-produced cytokines in driving aggrecanases, matrix metalloproteinases, and other destructive and inflammatory responses in osteoarthritis. Arthritis Research & Therapy. 2006;8:R187. [PubMed: 17177994]

[18]. Badlani N, Oshima Y, Healey R, Coutts R, Amiel D. Use of bone morphogenic protein-7 as a treatment for osteoarthritis. Clinical Orthopaedics and Related Research. 2009;467:3221–3229. [PubMed: 18941854]

[19]. Hong JH, Lee GT, Lee JH, Kwon SJ, Park SH, Kim SJ, et al. Effect of bone morphogenetic protein-6 on macrophages. Immunology. 2009;128:e442–450. [PubMed: 19191909]

[20]. Li C, Zheng Z. What's the future of osteoarthritis treatment. Acta Scientific Orthopaedics. 2018;1:01–02.

[21]. Li CS, Zhang X, Peault B, Jiang J, Ting K, Soo C, et al. Accelerated chondrogenic differentiation of human perivascular stem cells with NELL-1. Tissue Engeering Part A. 2016;22:272–285.

[22]. Li C, Jiang J, Zheng Z, Lee KS, Zhou Y, Chen E, et al. Neural EGFL-Like 1 is a downstream regulator of Runt-related transcription factor 2 in chondrogenic differentiation and maturation. The American Journal of Pathology. 2017;183:963–972.

[23]. Siu RK, Zara JN, Hou Y, James AW, Kwak J, Zhang X, et al. NELL-1 promotes cartilage regeneration in an *in vivo* rabbit model. Tissue Engeering Part A. 2012;18:252–261.

[24]. Li CS, Zheng Z, Jiang J, Jiang WL, Lee K, Berthiaume EA, et al. Neural EGFL-Like 1 regulates cartilage maturation through Runt-related transcription factor 3-mediated Indian Hedgehog signaling. The American Journal of Pathology. 2018;188:392–403. [PubMed: 29137952]

[25]. Li CS, Zheng Z, Zhang XL, Asatrian G, Chen E, Song R, et al. Nfatc1 is a functional transcriptional factor mediating NELL-1-induced runx3 upregulation in chondrocytes. Internatinal Journal of Molecular Sciences. 2018;19 (1), 168.

[26]. Bartolome N, Szczypiorska M, Sanchez A, Sanz J, Juanola-Roura X, Gratacos J, et al. Genetic polymorphisms inside and outside the MHC improve prediction of as radiographic severity in addition to clinical variables. Rheumatology. 2012;51:1471–1478. [PubMed: 22495925]

[27]. Ho P, Bowes J, Filer CE, Bruce IN, Barton A. Investigation of Crohn's disease and ankylosing spondylitis susceptibility loci with psoriatic arthritis. Arthritis And Rheumatism. 2008;58:S350–S350.

[28]. Polo YLBJ, Szczypiorska M, Bartolome N, Campos J, Flores-Robles BJ, Sanz J, et al. Clinical and genetic characteristics of ankylosing spondylitis patients with peripheral arthritis at disease onset. Clinical and Experimental Rheumatology. 2019;37 (2):0215–0221.

[29]. Klingenhoff A, Frech K, Quandt K, Werner T. Functional promoter modules can be defected by formal models independent of overall nucleoside sequence similarity. Bioinformatics. 1999;15:180–186. [PubMed: 10222404]

[30]. Desai J, Shannon ME, Johnson MD, Ruff DW, Hughes LA, Kerley MK, et al. Nell1-deficient mice have reduced expression of extracellular matrix proteins causing cranial and vertebral defects. Human Molecular Genetics. 2006;15:1329–1341. [PubMed: 16537572]

[31]. Kuyinu EL, Narayanan G, Nair LS, Laurencin CT. Animal models of osteoarthritis: Classification, update, and measurement of outcomes. Journal of Orthopaedic Surgery and Research. 2016;11:19. [PubMed: 26837951]

[32]. Brust V, Schindler PM, Lewejohann L. Lifetime development of behavioural phenotype in the house mouse (Mus musculus). Frontiers In Zoology. 2015;12:S1–S17.

[33]. Shen J, James AW, Zhang X, Pang S, Zara JN, Asatrian G, et al. Novel Wnt regulator NELlike molecule-1 antagonizes adipogenesis and augments osteogenesis induced by bone morphogenetic protein 2. The American Journal of Pathology. 2016;186:419–434. [PubMed: 26772960]

[34]. Fukubayashi T, Kurosawa H. The contact area and pressure distribution pattern of the knee - a study of normal and osteoarthrotic knee joints. Acta Orthopaedica Scandinavica. 1980;51:871–879. [PubMed: 6894212]

[35]. van de Loo AA, van den Berg WB. Effects of murine recombinant interleukin 1 on synovial joints in mice: Measurement of patellar cartilage metabolism and joint inflammation. Annals of the Rheumatic Diseases. 1990;49:238–245. [PubMed: 2339905]

[36]. van Beuningen HM, van der Kraan PM, Arntz OJ, van den Berg WB. *In vivo* protection against interleukin-1-induced articular cartilage damage by transforming growth factor-beta 1: Age-related differences. Annals of the Rheumatic Diseases. 1994;53:593–600. [PubMed: 7979598]

[37]. Allen KD, Adams SB, Mata BA, Shamji MF, Gouze E, Jing LF, et al. Gait and behavior in an IL1βeta-mediated model of rat knee arthritis and effects of an IL1 antagonist. Journal of Orthopaedic Research. 2011;29:694–703. [PubMed: 21437948]

[38]. Vandeloo AAJ, Vandenberg WB. Effects of murine recombinant interleukin-1 on synovial joints in mice - measurement of patellar cartilage metabolism and joint inflammation. Annals of the Rheumatic Diseases. 1990;49:238–245. [PubMed: 2339905]

[39]. Kwak JH, Zhang YL, Park J, Chen E, Shen J, Chawan C, et al. Pharmacokinetics and osteogenic potential of Pegylated NELL-1 *in vivo* after systemic administration. Biomaterials. 2015;57:73–83. [PubMed: 25913252]

[40]. Lundberg C, Asberg I, Ionescu M, Reiner A, Smedegard G, Poole AR. Changes in cartilage proteoglycan aggrecan after intra-articular injection of interleukin-1 in rabbits: Studies of

synovial fluid and articular cartilage. Annals of the Rheumatic Diseases. 1996;55:525–534. [PubMed: 8774180]

[41]. Page Thomas DP, King B, Stephens T, Dingle JT. *In vivo* studies of cartilage regeneration after damage induced by catabolin/interleukin-1. Annals of the Rheumatic Diseases. 1991;50:75–80. [PubMed: 1998394]

[42]. Heilborn U, Berge OG, Arborelius L, Brodin E. Spontaneous nociceptive behaviour in female mice with Freund's complete adjuvant- and carrageenan-induced monoarthritis. Brain Research. 2007;1143:143–149. [PubMed: 17316576]

[43]. Lakes EH, Allen KD. Gait analysis methods for rodent models of arthritic disorders: Reviews and recommendations. Osteoarthritis And Cartilage. 2016;24:1837–1849. [PubMed: 26995111]

[44]. Amini P, Ettlin J, Opitz L, Clementi E, Malbon A, Markkanen E. An optimised protocol for isolation of RNA from small sections of laser-capture microdissected FFPE tissue amenable for next-generation sequencing. BMC Molecular Biology. 2017;18:22. [PubMed: 28835206]

[45]. Akkiraju H, Nohe A. Role of chondrocytes in cartilage formation, progression of osteoarthritis and cartilage regeneration. Journal of Developmental Biology. 2015;3:177–192. [PubMed: 27347486]

[46]. Kumar P, Banik S. Pharmacotherapy options in rheumatoid arthritis. Clinical Medicine Insights. Arthritis Musculoskeletal Disorders. 2013;6:35–43. [PubMed: 23997576]

[47]. Kapoor M, Martel-Pelletier J, Lajeunesse D, Pelletier JP, Fahmi H. Role of proinflammatory cytokines in the pathophysiology of osteoarthritis. Nature Reviews Rheumatology. 2011;7:33–42. [PubMed: 21119608]

[48]. Berenbaum F Osteoarthritis as an inflammatory disease (osteoarthritis is not osteoarthrosis!). Osteoarthritis And Cartilage. 2013;21:16–21. [PubMed: 23194896]

[49]. Sokolove J, Lepus CM. Role of inflammation in the pathogenesis of osteoarthritis: Latest findings and interpretations. Therapeutic Advances in Musculoskeletal Disease. 2013;5:77–94. [PubMed: 23641259]

[50]. Shlopov BV, Gumanovskaya ML, Hasty KA. Autocrine regulation of collagenase 3 (matrix metalloproteinase 13) during osteoarthritis. Arthritis And Rheumatism. 2000;43:195–205. [PubMed: 10643716]

[51]. Arend WP, Dayer JM. Inhibition of the production and effects of interleukin-1 and tumornecrosis-factor-alpha in rheumatoid-arthritis. Arthritis And Rheumatism. 1995;38:151–160. [PubMed: 7848304]

[52]. Pearson MJ, Herndler-Brandstetter D, Tariq MA, Nicholson TA, Philp AM, Smith HL, et al. IL-6 secretion in osteoarthritis patients is mediated by chondrocyte-synovial fibroblast cross-talk and is enhanced by obesity. Scientific Reports. 2017;7:3451. [PubMed: 28615667]

[53]. Goldring MB, Otero M. Inflammation in osteoarthritis. Current Opinion In Rheumatology. 2011;23:471–478. [PubMed: 21788902]

[54]. Wang MN, Sampson ER, Jin HT, Li J, Ke QH, Im HJ, et al. MMP13 is a critical target gene during the progression of osteoarthritis. Arthritis Research & Therapy. 2013;15:R5. [PubMed: 23298463]

[55]. Stanton H, Rogerson FM, East CJ, Golub SB, Lawlor KE, Meeker CT, et al. ADAMTS5 is the major aggrecanase in mouse cartilage *in vivo* and *in vitro*. Nature. 2005;434:648–652. [PubMed: 15800625]

[56]. van Beuningen HM, Stoop R, Buma P, Takahashi N, van der Kraan PM, van den Berg WB. Phenotypic differences in murine chondrocyte cell lines derived from mature articular cartilage. Osteoarthritis Cartilage. 2002;10:977–986. [PubMed: 12464558]

[57]. Tan YY, Zhao G, Wang D, Wang JM, Tang JR, Ji ZL. A new strategy of minimally invasive surgery for cholecystolithiasis: Calculi removal and gallbladder preservation. Digestive Surgury. 2013;30:466–471.

[58]. Gosset M, Berenbaum F, Thirion S, Jacques C. Primary culture and phenotyping of murine chondrocytes. Nature Protocols. 2008;3:1253–1260.

[59]. Krueger F, Andrews SR. Bismark: A flexible aligner and methylation caller for Bisulfite-Seq applications. Bioinformatics. 2011;27:1571–1572. [PubMed: 21493656]

[60]. Stockwell PA, Chatterjee A, Rodger EJ, Morison IM. DMAP: Differential methylation analysis package for RRBS and WGBS data. Bioinformatics. 2014;30:1814–1822. [PubMed: 24608764]

[61]. Benjamin DJ, Berger JO, Johannesson M, Nosek BA, Wagenmakers E- J, Berk R, et al. Redefine statistical significance. We propose to change the default p-value threshold for statistical significance from 0.05 to 0.005 for claims of new discoveries. Nature Human Behaviour. 2017;1.

[62]. Aubrey J Hough J. Pathology of osteoarthritis In: Moskowitz RW, Altman RD, Hochberg MC, Buckwalter JA, Goldberg VM, editors. Osteoarthritis: Diagnosis and medical/surgical management. 4th ed. Philadelphia, PA: Wolter Kluwer/Lippincott Willams & Wilkins; 2007 p. 51–72.

[63]. Liu CL, Bai YC, Ganea D, Hart RP. Species-specific activity of rat recombinant interleukin-1-beta. Journal Of Interferon And Cytokine Research. 1995;15:985–992. [PubMed: 8590311]

[64]. Koussounadis AI, Ritchie DW, Kemp GJL, Secombes CJ. Analysis of fish IL-1 beta and derived peptide sequences indicates conserved structures with species-specific IL-1 receptor binding: Implications for pharmacological design. Current Pharmaceutical Design 2004;10:3857–3871. [PubMed: 15579075]

[65]. Yano F, Hojo H, Ohba S, Fukai A, Hosaka Y, Ikeda T, et al. A novel disease-modifying osteoarthritis drug candidate targeting Runx1. Annals of the Rheumatic Diseases. 2013;72:748–753. [PubMed: 23041841]

[66]. Aini H, Itaka K, Fujisawa A, Uchida H, Uchida S, Fukushima S, et al. Messenger RNA delivery of a cartilage-anabolic transcription factor as a disease-modifying strategy for osteoarthritis treatment. Scientific Reports. 2016;6:18743. [PubMed: 26728350]

[67]. Greenblatt MB, Ritter SY, Wright J, Tsang K, Hu D, Glimcher LH, et al. NFATc1 and NFATc 2 repress spontaneous osteoarthritis. Proceedings of the National Academy of Sciences of the United States of America. 2013;110:19914–19919. [PubMed: 24248346]

[68]. Beier F NFATs are good for your cartilage! Osteoarthritis And Cartilage. 2014;22:893–895. [PubMed: 24769231]

[69]. Snelling S, Rout R, Davidson R, Clark I, Carr A, Hulley PA, et al. A gene expression study of normal and damaged cartilage in anteromedial gonarthrosis, a phenotype of osteoarthritis. Osteoarthritis Cartilage. 2014;22:334–343. [PubMed: 24361742]

[70]. Oegema TR, Carpenter RJ, Hofmeister F, Thompson RC. The interaction of the zone of calcified cartilage and subchondral bone in osteoarthritis. Microscopy Research And Technique. 1997;37:324–332. [PubMed: 9185154]

[71]. Candela ME, Yasuhara R, Iwamoto M, Enomoto-Iwamoto M. Resident mesenchymal progenitors of articular cartilage. Matrix Biology. 2014;39:44–49. [PubMed: 25179676]

[72]. James AW, Shen J, Zhang X, Asatrian G, Goyal R, Kwak JH, et al. NELL-1 in the treatment of osteoporotic bone loss. Nature Communications. 2015;6:7362.

[73]. Ranger AM, Gerstenfeld LC, Wang J, Kon T, Bae H, Gravallese EM, et al. The nuclear factor of activated t cells (NFAT) transcription factor NFATp (NFAT2) is a repressor of chondrogenesis. The Journal of Experimental Medicine. 2000;191:9–22. [PubMed: 10620601]

[74]. Wang J, Gardner BM, Lu Q, Rodova M, Woodbury BG, Yost JG, et al. Transcription factor Nfat1 deficiency causes osteoarthritis through dysfunction of adult articular chondrocytes. The Journal of Pathology. 2009;219:163–172. [PubMed: 19526482]

[75]. Yoo SA, Park BH, Yoon HJ, Lee JY, Song JH, Kim HA, et al. Calcineurin modulates the catabolic and anabolic activity of chondrocytes and participates in the progression of experimental osteoarthritis. Arthritis And Rheumatism. 2007;56:2299–2311. [PubMed: 17599750]

[76]. Miclea RL, Siebelt M, Finos L, Goeman JJ, Lowik CW, Oostdijk W, et al. Inhibition of Gsk3β in cartilage induces osteoarthritic features through activation of the canonical Wnt signaling pathway. Osteoarthritis Cartilage. 2011;19:1363–1372. [PubMed: 21911068]

[77]. Yaykasli KO, Oohashi T, Hirohata S, Hatipoglu OF, Inagawa K, Demircan K, et al. ADAMTS9 activation by interleukin 1β via NFATc1 in OUMS-27 chondrosarcoma cells and in human chondrocytes. Molecular and Cellular Biochemistry. 2009;323:69–79. [PubMed: 19052845]

[78]. Jeffries MA, Donica M, Baker LW, Stevenson ME, Annan AC, Humphrey MB, et al. Genome-wide DNA methylation study identifies significant epigenomic changes in osteoarthritic cartilage. Arthritis & Rheumatology. 2014;66:2804–2815. [PubMed: 24980887]

[79]. Wang Y, Godec J, Ben-Aissa K, Cui KR, Zhao KJ, Pucsek AB, et al. The transcription factors T-bet and Runx are required for the ontogeny of pathogenic interferon-γ-producing T helper 17 cells. Immunity. 2014;40:355–366. [PubMed: 24530058]

[80]. Tokuhiro S, Yamada R, Chang XT, Suzuki A, Kochi Y, Sawada T, et al. An intronic SNP in a RUNX1 binding site of SLC22A4, encoding an organic cation transporter, is associated with rheumatoid arthritis. Nature Genetics. 2003;35:341–348. [PubMed: 14608356]

[81]. Johnson K, Zhu ST, Tremblay MS, Payette JN, Wang JN, Bouchez LC, et al. A stem cell-based approach to cartilage repair. Science. 2012;336:717–721. [PubMed: 22491093]

[82]. Blanco FJ, Ruiz-Romero C. New targets for disease modifying osteoarthritis drugs: Chondrogenesis and Runx1. Annals of the Rheumatic Diseases. 2013;72:631–634. [PubMed: 23444194]

[83]. Li C, Zheng Z, Ha P, Chen X, Jiang W, Sun S, et al. Neurexin superfamily cell membrane receptor contactin-associated protein like-4 (Cntnap4) is involved in neural EGFL-like 1 (NELL-1)-responsive osteogenesis. Journal of Bone and Mineral Research. 2018;33:1813–1825. [PubMed: 29905970]

[84]. Alarcon-Riquelme ME. Role of RUNX in autoimmune diseases linking rheumatoid arthritis, psoriasis and lupus. Arthritis Research & Therapy. 2004;6:169–173. [PubMed: 15225361]

[85]. Lee YH, Bae SC, Kim JH, Seo YH, Choi SJ, Ji JD, et al. Meta-analysis of SLC22A4 and RUNX1 polymorphisms associations with rheumatoid arthritis susceptibility. Zeitschrift Fur Rheumatologie. 2015;74:351–358. [PubMed: 24972750]

[86]. Gregory MH, Capito N, Kuroki K, Stoker AM, Cook JL, Sherman SL. A review of translational animal models for knee osteoarthritis. Arthritis. 2012;2012:764621. [PubMed: 23326663]

[87]. Punzi L, Galozzi P, Luisetto R, Favero M, Ramonda R, Oliviero F, et al. Post-traumatic arthritis: Overview on pathogenic mechanisms and role of inflammation. RMD Open. 2016;2.

[88]. Proffen BL, McElfresh M, Fleming BC, Murray MM. A comparative anatomical study of the human knee and six animal species. Knee. 2012;19:493–499. [PubMed: 21852139]

Group	Treatment	
Control	6 μl PBS for 7 days	6 μl PBS for 7 days
NELL-1	6 μl PBS for 7 days	2 μg NELL-1 in 6 μl PBS for 7 days
IL1β	100 ng IL1β in 6 μl PBS for 7 days	100 ng IL1β in 6 μl PBS for 7 days
IL1β + NELL-1	100 ng IL1β in 6 μl PBS for 7 days	100 ng IL1β + 2 μg NELL-1 in 6 μl PBS for 7 days

Fig. 1. Schematic depicting the intra-articular injection animal model.
'Control' group: 6 μl PBS per injection for 14 days; 'NELL-1' group: 6 μl PBS per injection for 7 days followed by 2 μg recombinant human NELL-1 in 6 μl PBS per injection for the next 7 days; 'IL1β' group: 100 ng recombinant human IL1β in 6 μl PBS per injection for 14 days; and 'IL1β + NELL-1' group: 100 ng IL1β in 6 μl PBS per injection for 7 days to trigger inflammation, and 100 ng IL1β + 2 μg NELL-1 in 6 μl PBS per injection for the next 7 days. All injections were performed twice daily.
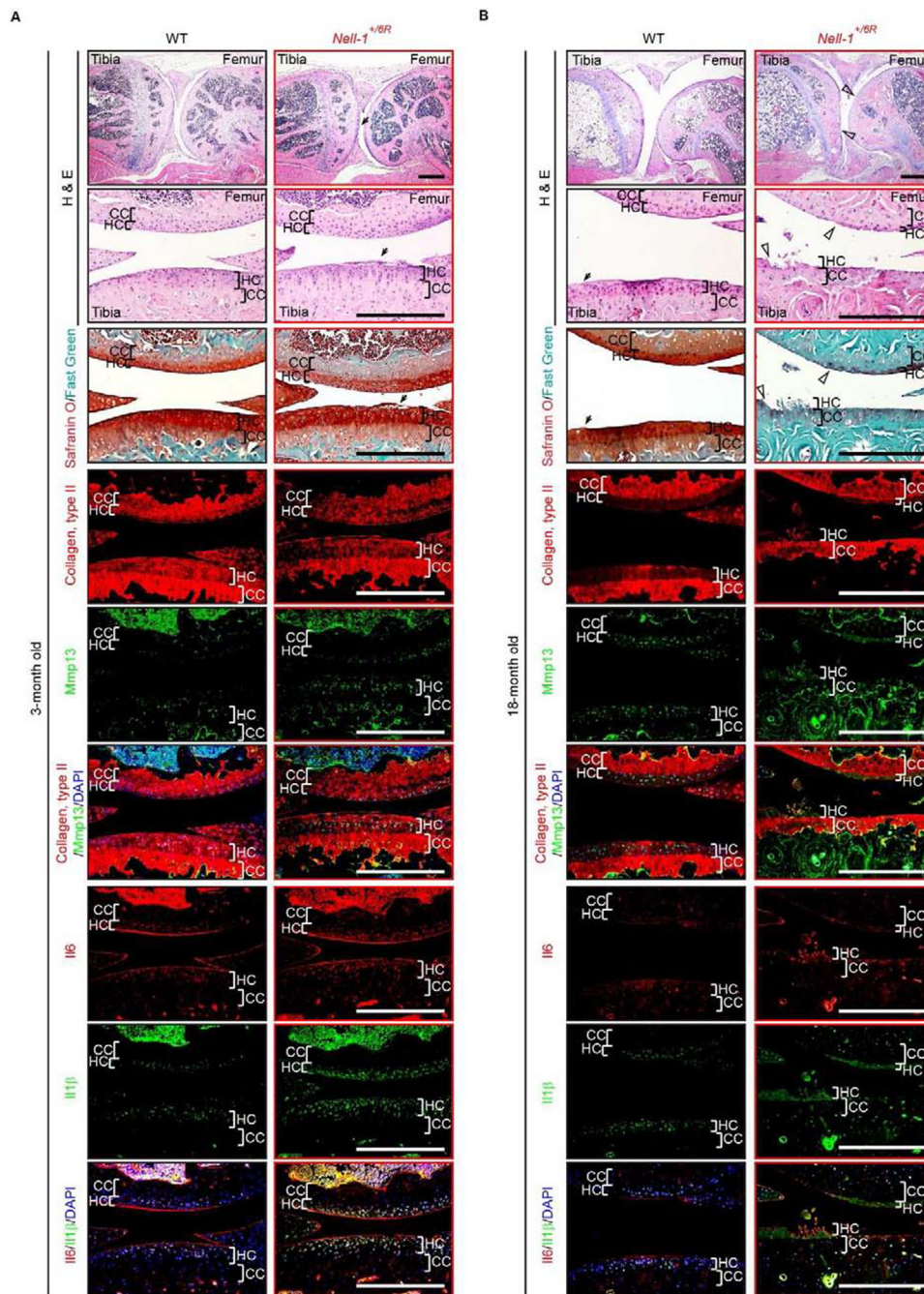
Fig. 2. Characterization of WT and *Nell-1*-haploinsufficient (*Nell-1*$^{+/6R}$) mouse knee joints at 3 and 18 months of age.

Representative photos of 3- (**A**), and 18-month- (**B**) old female WT and *Nell-1*$^{+/6R}$ mouse knee joints. H&E staining was performed for histological analysis, while safranin O was used to stain proteoglycans. Expression of anabolic marker type II collagen (Collagen, type II), catabolic marker Mmp13, as well as proinflammatory markers interleukin (Il)1β and Il6 was evaluated by IF staining. DAPI was used for nuclear counterstaining. HC: uncalcified hyaline zone of articular cartilage; CC: calcified zone of articular cartilage. Solid arrows

indicate the erosion in HC; open triangles indicate severe loss of HC. Bar = 500 μm. Relative RNA expression in the tibial cartilage is presented in Supplementary Fig. 5.
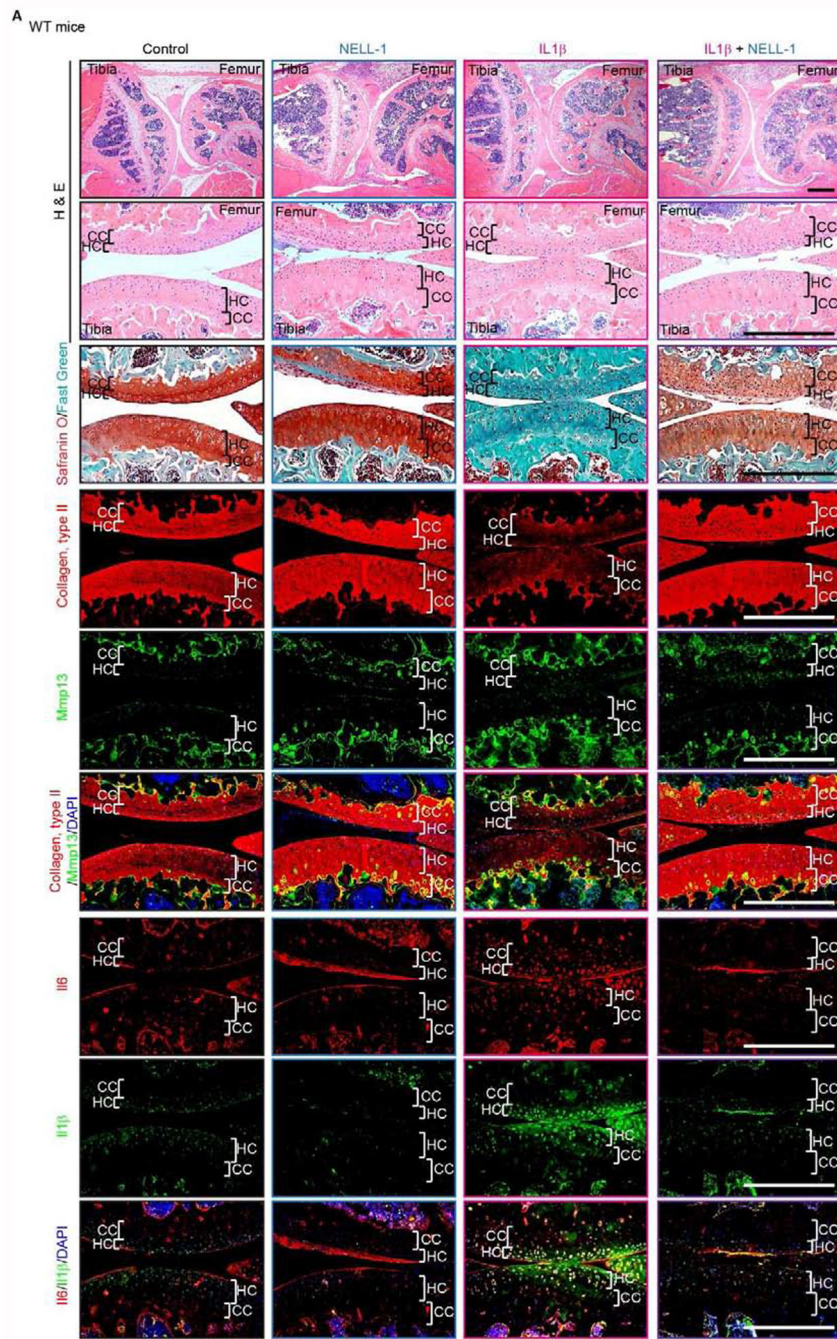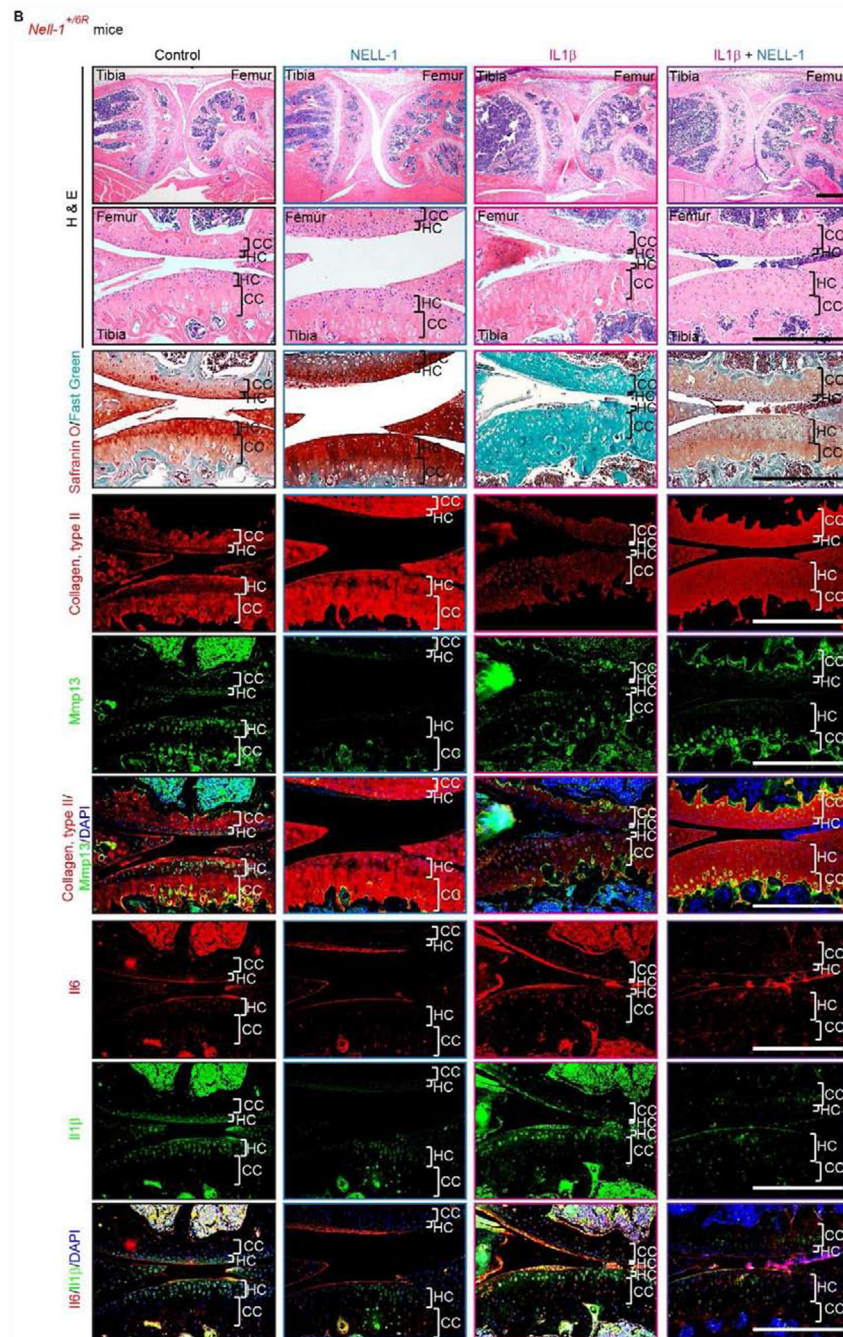
Fig. 3. Characterization of mouse knee joints after 14 days of intra-articular injections.
Representative photos of 2.5-month-old female WT (**A**) and *Nell-1*^{+/6R} (**B**) mouse knee
joints after 14 days of intra-articular injections (3 months old at the end of treatment). The
injection schematic of each group is presented in Fig. 1. H&E staining was performed for
histological analysis, while safranin O was used to stain proteoglycans. Expression of
Collagen, type II, Mmp13, Il1β, and Il6 was evaluated by IF staining. DAPI was used for
nuclear counterstaining. HC: uncalcified hyaline zone of articularx cartilage; CC: calcified
zone of articular cartilage. Relative RNA expression in the tibial cartilage is presented in

Supplementary Fig. 7, while gait scores are summarized in Supplementary Fig. 8. Corresponding videos of *Nell-1^{+/6R}* mice (**B**) are provided in Supplementary Videos 1–7. Bar = 500 μm.
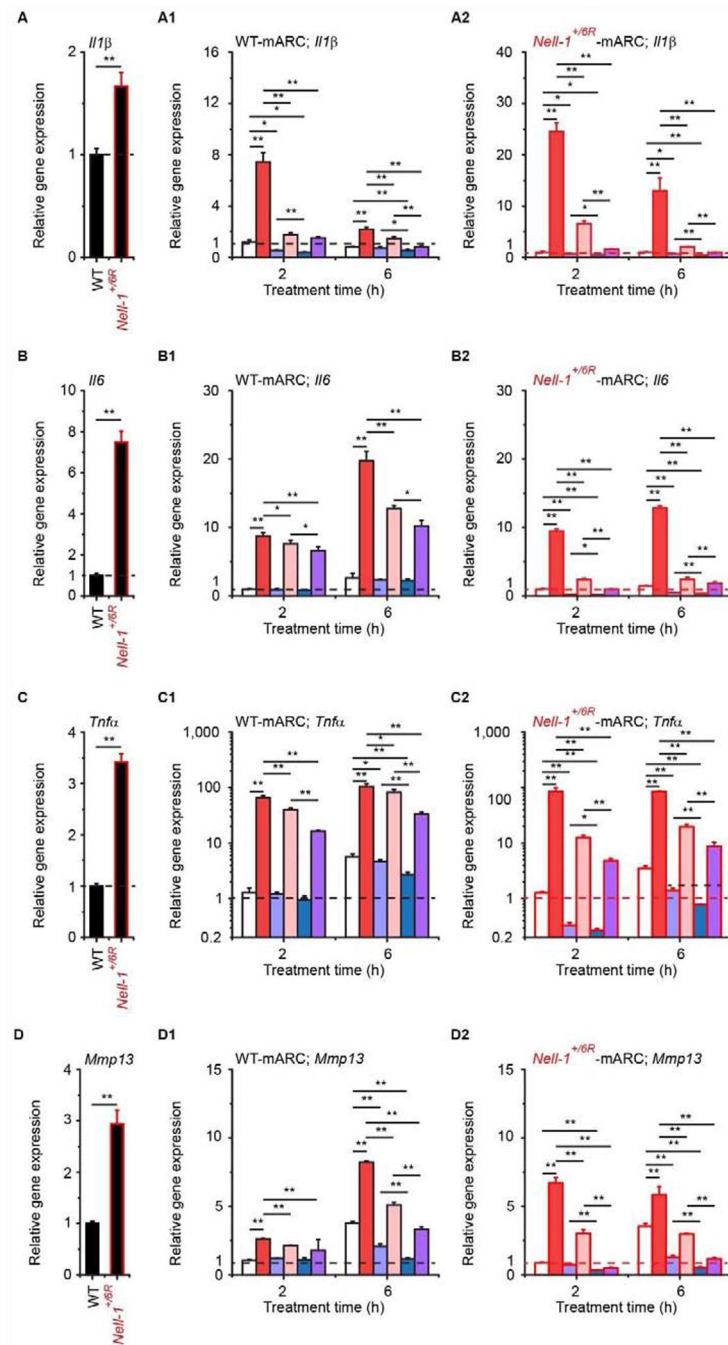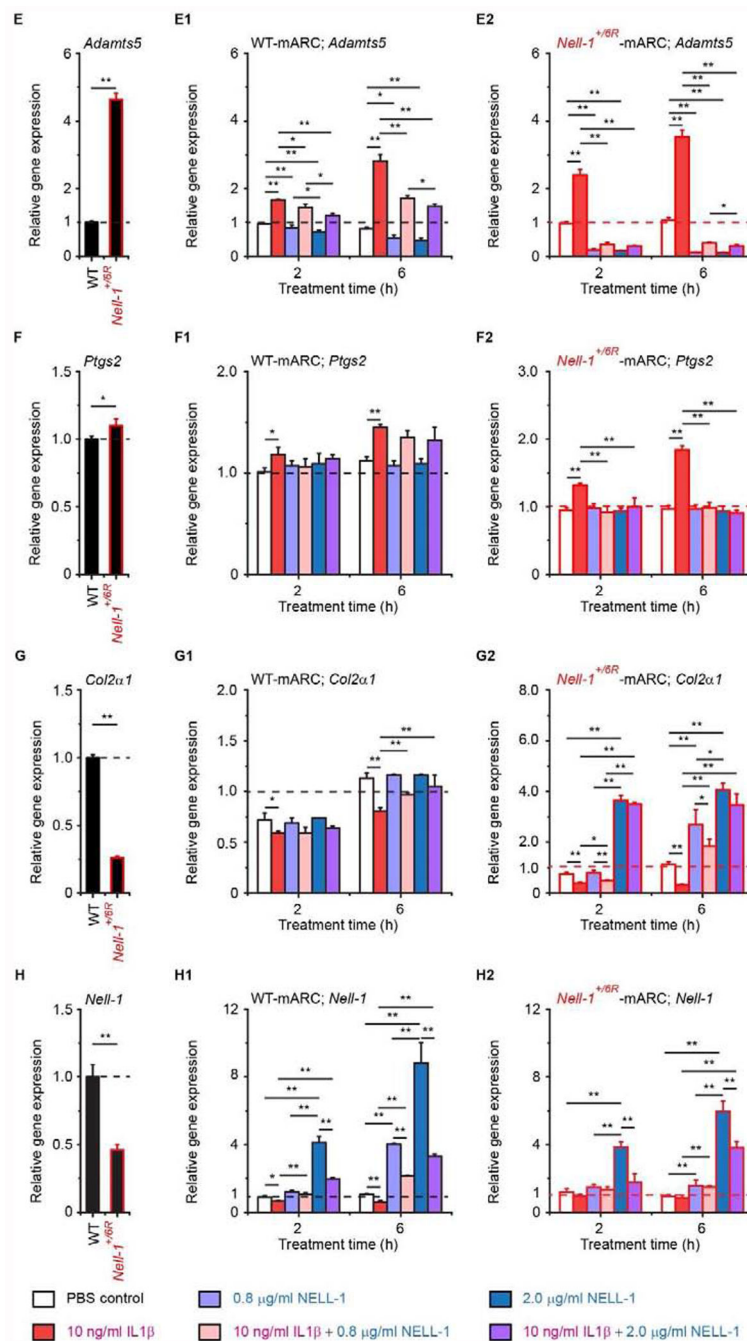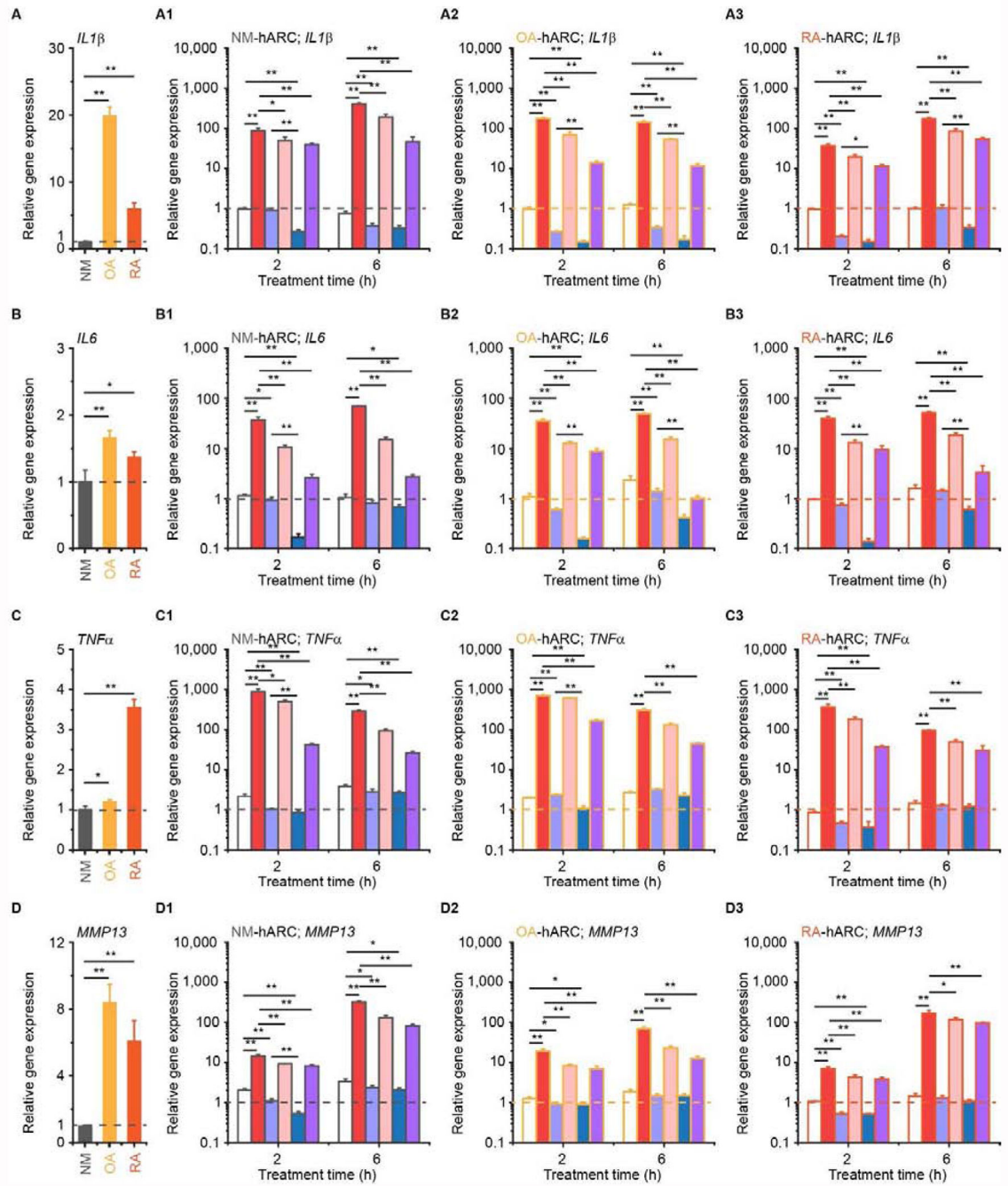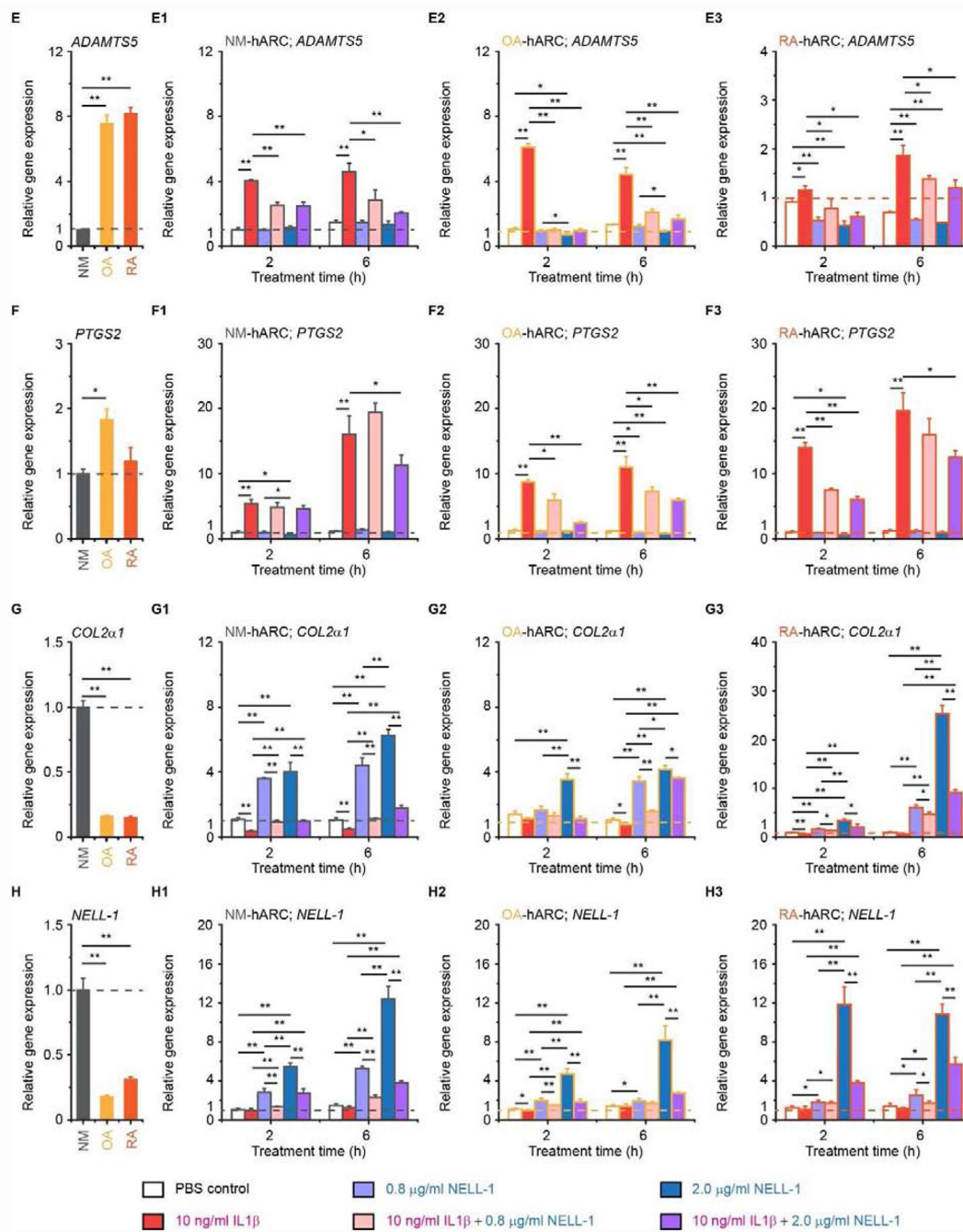
Fig. 4. Effects of NELL-1 on gene expression in primary mouse articular chondrocytes (mARCs).
Expression of *Il1β* (**A-A2**), *Il6* (**B-B2**), *Tnfβ* (**C-C2**), *Mmp13* (**D-D2**), *Adamts5* (**E-E2**),
Ptgs2 (**F-F2**), *Col2α1* (**G-G2**), and *Nell-1* (**H-H2**) was quantified by real-time PCR, and the
data were normalized to the respective levels of WT-mARCs (**A-H** and **A1-H1**) or
Nell-1^{+/6R}-mARCs (**A2-H2**) before treatment (dashed lines). Mean + SD of three
independent experiments performed in duplicate are shown. One-way ANOVA and two-
sample *t*-test analyses were performed. *, $P < 0.05$, a suggestive difference; **, $P < 0.005$, a
statistically significant difference.

Fig. 5. Effects of NELL-1 on gene expression in primary human articular chondrocytes (hARCs). Expression of *IL1β* (**A-A3**), *IL6* (**B-B3**), *TNFa* (**C-C3**), *MMP13* (**D-D3**), *ADAMTS5* (**E-E3**), *PTGS2* (**F-F3**), *COL2a1* (**G-G3**), and *NELL-1* (**H-H3**) was quantified by real-time PCR, and the data were normalized to the respective levels of pathological normal/health (NM)-hARCs (**A-H** and **A1-H1**), osteoarthritis (OA)-hARCs (**A2-H2**), or rheumatoid arthritis (RA)-hARCs (**A3-H3**) before treatment (dashed lines). Mean + SD of three independent experiments performed in duplicate are shown. One-way ANOVA and two-
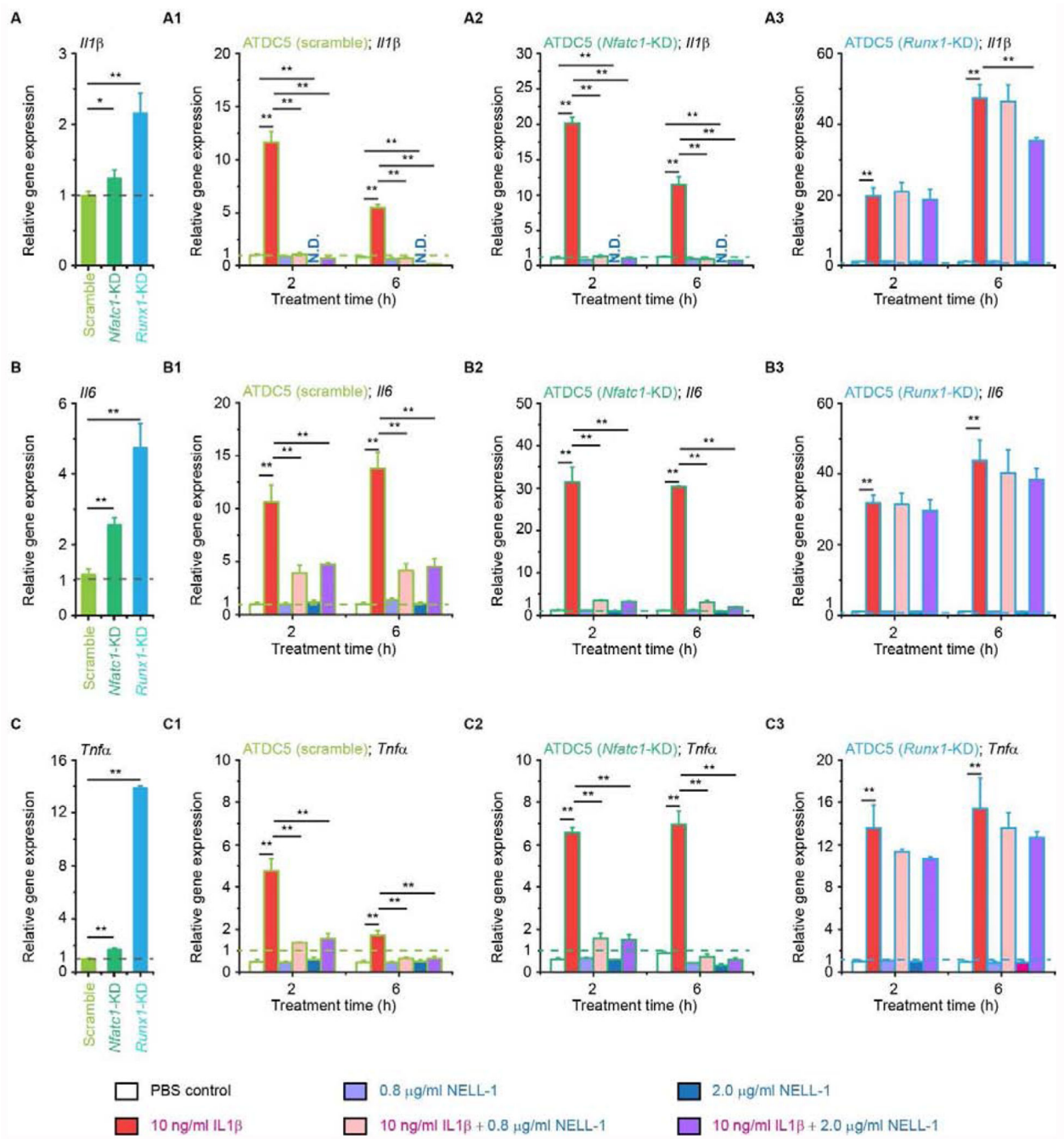
sample t-test analyses were performed. *, $P < 0.05$, a suggestive difference; **, $P < 0.005$, a statistically significant difference.

Fig. 6. Effects of *Nfatc1*- and *Runx1*-KD on NELL-1's anti-inflammatory potency.
Stable scramble, *Nfatc1*-, and *Runx1*-KD ATDC5 clones were established (Supplementary
Fig. 13). Expression of proinflammatory genes *Il1β* (**A-A3**), *Il6* (**B-B3**), and *Tnfα* (**C-C3**)
was quantified by real-time PCR, and the data were normalized to the respective levels of
ATDC5 (**A-C**), ATDC5 (scramble) (**A1-C1**), ATDC5 (*Nfatc1*-KD) (**A2-C2**), or ATDC5
(*Runx1*-KD) (**A3-C3**) cells before treatment (dashed lines). Mean + SD of three independent
experiments performed in duplicate are shown. One-way ANOVA and two-sample *t*-test

analyses were performed. N.D.: not detectable. *, $P < 0.05$, a suggestive difference; **, $P <$ 0.005, a statistically significant difference.
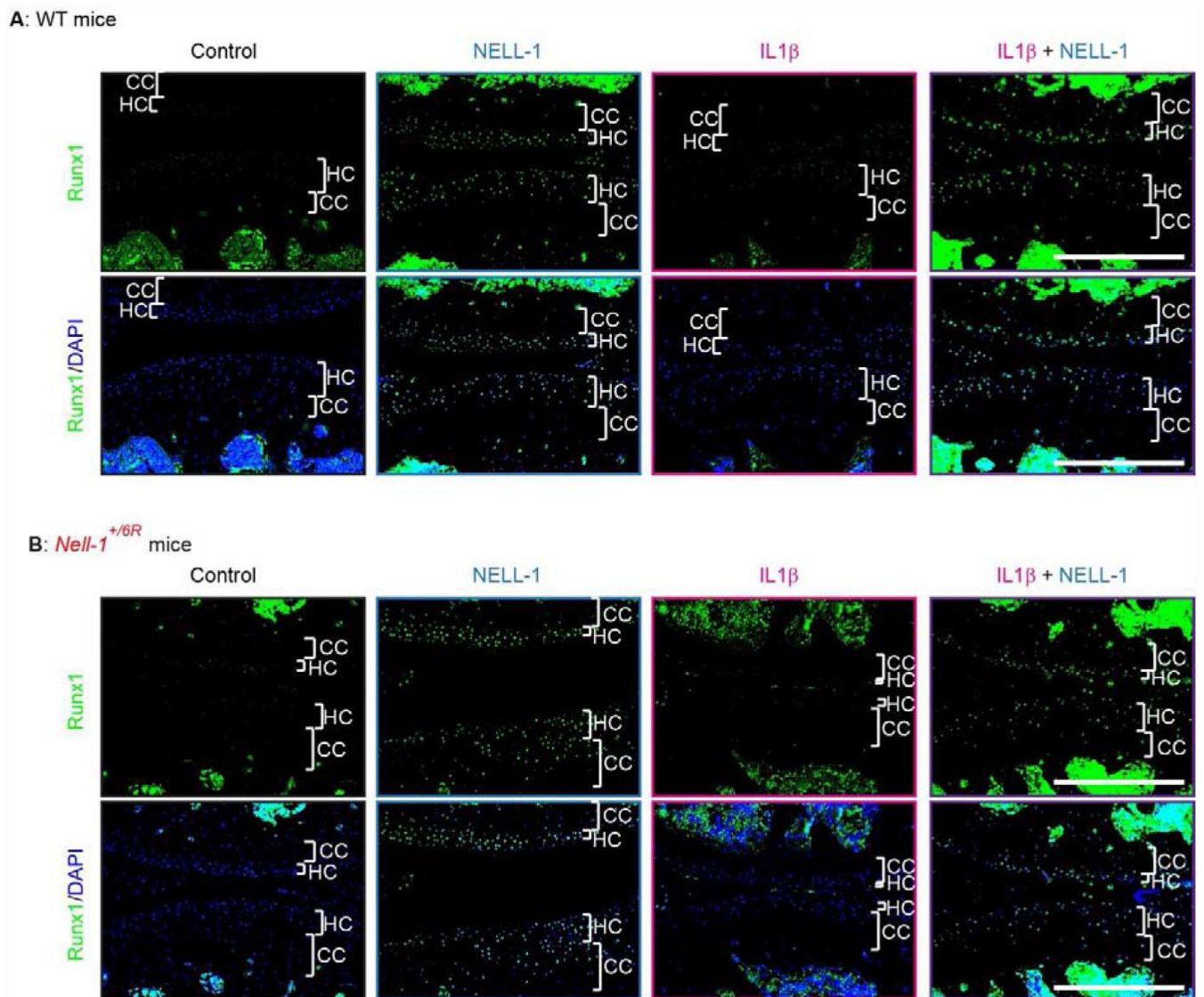
Fig. 7. Expression of Runx1 in mouse knees with intra-articular NELL-1 administration.
Using IF, Runx1 expression was observed in 2.5-month-old female WT (**A**) and *Nell-1*$^{+/6R}$
(**B**) mouse knee joints after 14 days of intra-articular injections (3 months old at the end of treatment). DAPI was used for nuclear counterstaining. HC: uncalcified hyaline zone of articular cartilage; CC: calcified zone of articular cartilage. Bar = 500 μm.
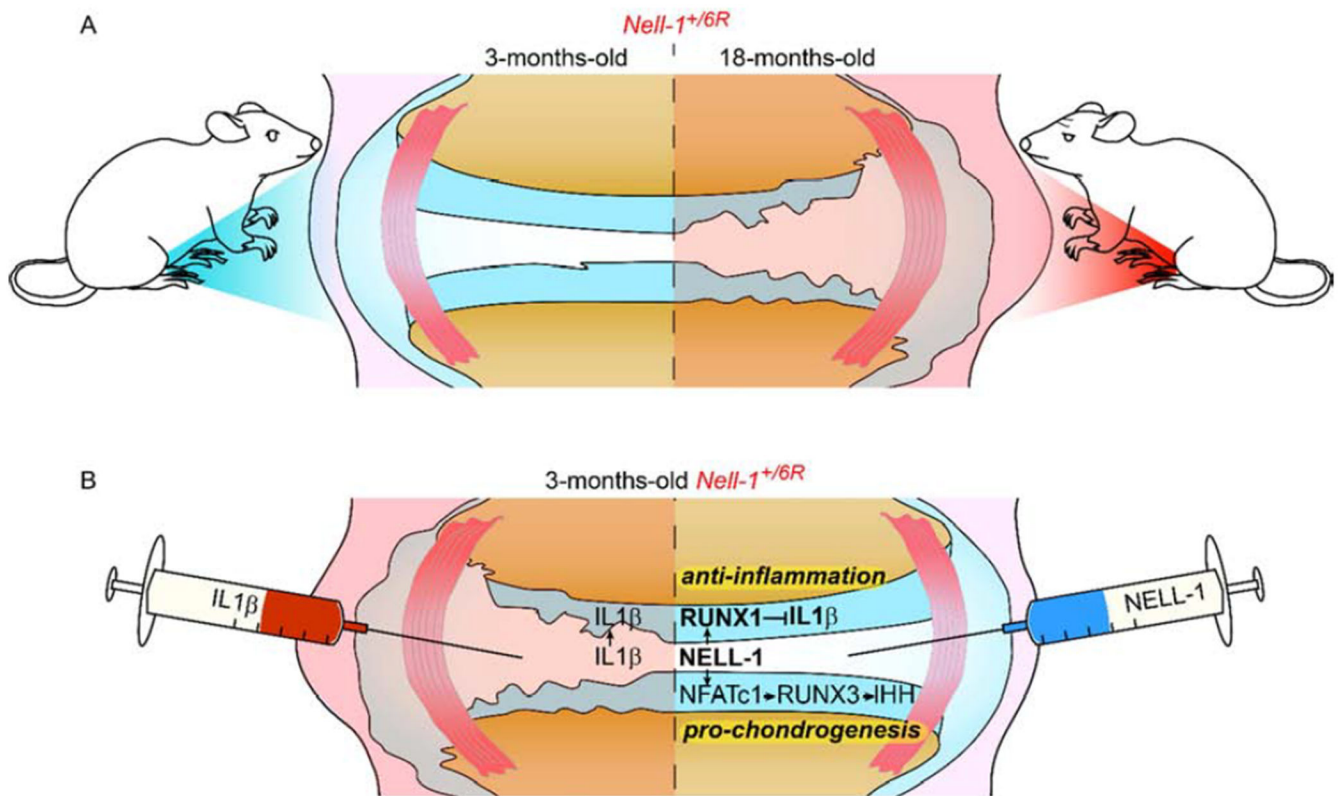
Fig. 8. Schematic depicting NELL-1's effects in articular cartilage.
(**A**) Focal wear and tear of HC with early chondrocyte clustering became evident in the tibial plateau cartilage of 3-month-old *Nell-1$^{+/6R}$* mice, while severe loss of HC was observed in the knees of 18-month-old *Nell-1$^{+/6R}$* mice. (**B**) Our previous studies revealed that the NELL-1 → NFATc1 → RUNX3 → IHH cascade in chondrocytes is responsible for NELL-1's pro-chondrogenic bioactivities. Here, we demonstrate that RUNX1, instead of NFATc1, is essential for NELL-1 to exhibit its anti-inflammatory properties in chondrocytes.